Aus der Klinik für Dermatologie, Venerologie und Allergologie
(Prof. Dr. med. M. P. Schön)
der Medizinischen Fakultät der Universität Göttingen

The α_E(CD103)β_7 integrin and its role on regulatory T-cells in allergic contact dermatitis

INAUGURAL-DISSERTATION

zur Erlangung des Doktorgrades
der Medizinischen Fakultät der
Georg-August-Universität zu Göttingen

vorgelegt von

Jan-Hendrik Bernhard Hardenberg

aus

Friesoythe

Berlin, 30.12.2019

Dekan:	Prof. Dr. med. W. Brück
Referent	Prof. Dr. med. M. P. Schön
Korreferent/in:	Prof. Dr. Jürgen Wienands
Drittreferent/in:	Prof. Dr. Thomas Meyer

Datum der mündlichen Prüfung: 05.11.2020

Hiermit erkläre ich, die Dissertation mit dem Titel "The α_E(CD103)β_7 integrin and its role on regulatory T-cells in allergic contact dermatitis" eigenständig angefertigt und keine anderen als die von mir angegebenen Quellen und Hilfsmittel verwendet zu haben.

Berlin, den …… ……

(Unterschrift)

Die Daten, auf denen die vorliegende Arbeit basiert, wurden teilweise publiziert:

Braun A, Dewert N, Brunnert F, Schnabel V, Hardenberg J-H, Richter B, Zachmann K, Cording S, Claßen A, Brans R et al. (2015): Integrin αE(CD103) Is Involved in Regulatory T-Cell Function in Allergic Contact Hypersensitivity. J Invest Dermatol 135, 2982–2991

Table of contents

List of figures

List of tables

List of non-standard abbreviations

ACD	Allergic contact dermatitis
Ag	Antigen
APC	Allophycocyanin
ATP	Adenosine triphosphate
BAC	Bacterial artificial chromosome
CCR	C-C chemokine receptor
CD	Cluster of differentiation
CFSE	Carboxyfluorescein succinimidyl ester
CHS	Contact hypersensitivity
CTLA	Cytotoxic T lymphocyte-associated protein
CXCL	Chemokine (C-X-C motif) ligand
DAMP	Danger-associated molecular pattern
DC	Dendritic cell
DEREG	Depletion of regulatory T-cells
dLN	Draining lymph node
DNA	Deoxyribonucleic acid
DT	Diphtheria toxin
DTR	Diphtheria toxin receptor
eGFP	Enhanced green fluorescent protein
ETM	Ear thickness measurement
FACS	Fluorescence-activated cell scanning
FCS	Fetal calf serum
FSC	Forward scatter
FoxP3	Forkhead box P3
IL	Interleukin
ILC	Innate lymphoid cell
KC	Keratinocyte
LAG	Lymphocyte activation gene
LN	Lymph node
MACS	Magnetic cell separation
MC	Mast cell
MHC	Major histocompatibility complex
MFI	Mean fluorescence intensity
OXA	Oxazolone
PE	Phycoerythrin
PerCP	Peridinin-chlorophyll-protein
PBS	Phosphate-buffered saline
RPM	Rounds per minute
PRR	Pattern recognition receptor
SD	Standard deviation
SEM	Standard error of the mean
SSC	Sideward scatter
Tc	Cytotoxic T-cell
TCR	T-cell receptor
T_{EFF}	T effector cell
TGF	Transforming growth factor
TNF	Tumor necrosis factor
Treg	Regulatory T-cell
wt	Wildtype

1 Introduction

1.1 Allergic contact dermatitis

Allergic contact dermatitis (ACD) is an inflammatory skin disorder caused by a type IV delayed hypersensitivity reaction (Coombs and Gell classification) directed against certain molecules, so called contact allergens, at the site of skin exposure. Clinically, ACD typically manifests in the form of eczematous lesions. An acute form and a chronic form can be differentiated. The acute form features erythema, itching and in more severe cases blisters and pain, whereas chronic eczema shows lichenification (thickening of skin folds), hyperkeratosis and rhagades. The chronic form is the consequence of continuous and repetitive exposure to the triggering contact allergen (Brasch et al. 2014). The hands are the most commonly affected body part, followed by the face (Uter et al. 2009; Reduta et al. 2013). Diagnosis of ACD is based on the clinical presentation, the medical history and epicutaneous testing to identify the allergen. ACD must be distinguished from other causes of eczema such as atopic dermatitis and irritant contact dermatitis.

ACD has a tremendous societal relevance, due to its high prevalence and its enormous role in occupational health. The German health survey from 1998 estimates the lifetime prevalence of actual diagnosed ACD at 15% and the 1-year prevalence at 7% (Brasch et al. 2014). This translates to almost 6 million patients a year diagnosed with ACD in Germany. The prevalence of sensitization to at least one allergen in western European countries is even higher at about 20% (Thyssen et al. 2007). In Germany, occupational skin diseases are by far the most frequently reported occupational disease with a proportion of 30% of all reported occupational diseases (Bundesanstalt für Arbeitsschutz und Arbeitsmedizin 2016). A study conducted in Bavaria found ACD to be the root cause of 57.5% of occupational skin disease cases (Dickel et al. 2001).

1.2 Pathophysiology of allergic contact dermatitis

ACD is generally regarded to be driven mainly by the adaptive immune system. However, this exclusive and simplified perspective does not hold up to closer scrutiny because innate and adaptive immune mechanisms contribute to the pathophysiology of ACD in a closely intertwined manner. Based on different underlying immune events, two phases are usually distinguished and discussed separately. The sensitization phase follows the first encounter of the immune system with the contact allergen. The effector phase refers to the inflammatory response initiated by re-exposure to the allergen. The latter phase is also called elicitation or challenge

phase. While the sensitization phase is clinically largely inapparent, the effector reaction elicits a dermatitis. The experimental model of ACD is commonly referred to as contact hypersensitivity (CHS) model, as is the case in this thesis.

1.2.1 Sensitization phase

1.2.1.1 Penetration of the skin barrier

The first step in sensitization is the penetration of the skin barrier by the contact allergen. The skin barrier is made up of several defense lines. The main defense against chemicals is the *stratum corneum* (Madison 2003), in which the intercellular space is filled with lipids that serve as a hydrophobic seal (Proksch et al. 2008). Tight junctions in the *stratum granulosum* are another important defense mechanism, restricting the passage of larger molecules through the tight interconnection of cells (Furuse et al. 2002; Baroni et al. 2012; Bäsler and Brandner 2017). Contact allergens overcome these defenses through lipophilicity and small size (Bos and Meinardi 2000). The vast majority of sensitizing agents have a molecular weight of less than 500 Dalton (<500 Dalton rule) (Bos and Meinardi 2000). In fact, the sensitization potential of chemicals can be predicted based upon their hydrophobicity and reactivity (Chipinda et al. 2011).

1.2.1.2 The haptenic nature of contact allergens

As a consequence of their small size, contact allergens are haptens by nature, meaning they are too small (<500 Dalton) to be directly recognized as antigens. To become immunogenic, they must first bind to proteins or peptides, a process termed haptenation (Figure 1, step 1) (Landsteiner and Jacobs 1936). Haptens are generally electrophilic and form hapten-protein conjugates through covalent binding to nucleophilic residues through electrophilic attack (Divkovic et al. 2005; Chipinda et al. 2011). The resulting hapten-protein conjugates act as foreign antigens and consecutively elicit an adaptive immune response (Figure 1, step 2). It has been firmly well established that haptens are part of the antigenic determinant recognized by the T-cell receptor (TCR) (Griem et al. 1996; Weltzien et al. 1996). The exact mechanisms of how dendritic cells (DCs) take up, process and eventually present hapten-protein conjugates are not entirely clear.

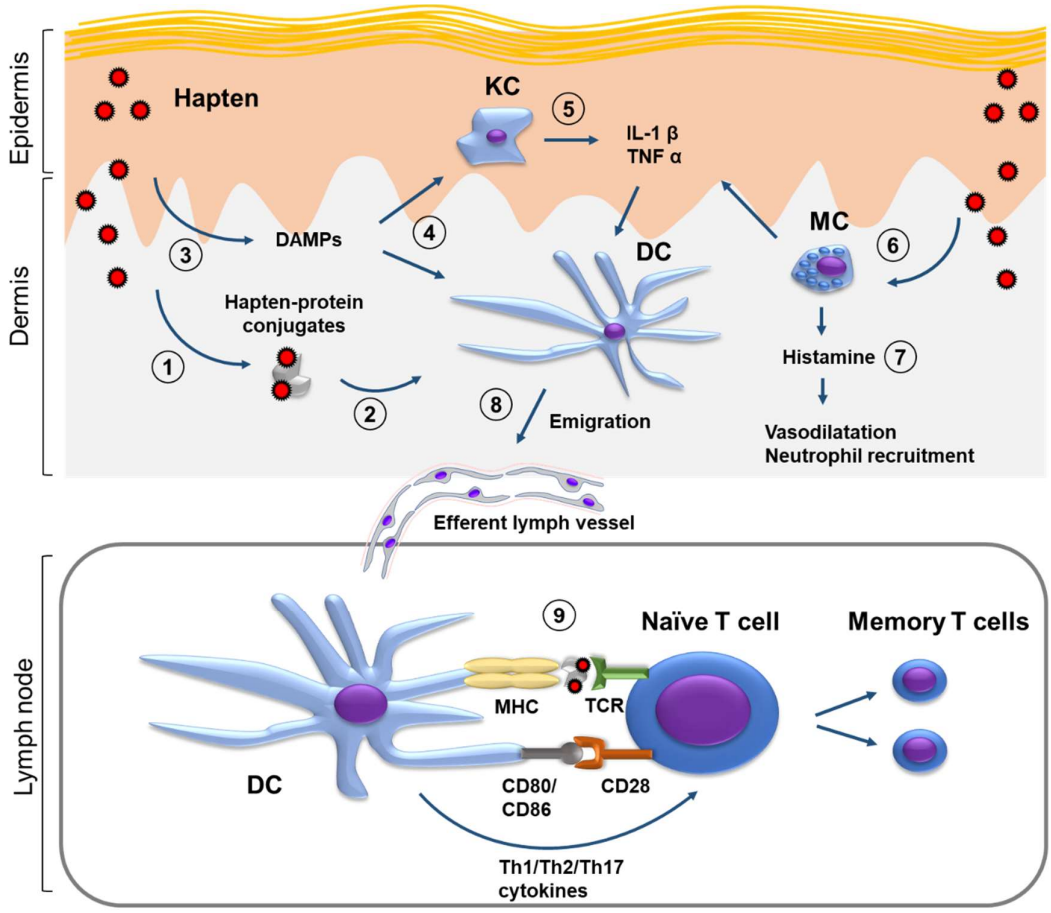

Figure 1: Early events in the sensitization phase
Haptens react with skin resident proteins to form hapten-protein conjugates (1). These hapten-protein conjugates are recognized as foreign antigens by dendritic cells (DCs), taken up, processed and loaded onto major histocompatibility complex (MHC) molecules (2). At the same time, haptens induce the formation of danger-associated molecular patterns (DAMPs) (3). These DAMPs activate both keratinocytes (KCs) and DCs through pattern recognition receptors (PPRs) (4). DC activation initiates emigration to the draining lymph node. Activated KCs contribute to DC activation through release of proinflammatory cytokines, mainly interleukin (IL)-1β and tumor necrosis factor (TNF) α (5). Mast cells (MCs) are directly activated by haptens and are another source of IL-1β and TNFα. (6) Additionally, MCs release histamine (7), which induces dilation of cutaneous blood vessel and promotes neutrophil recruitment. In the lymph node (8), DCs present MHC-bound antigens to naïve T-cells (9). The necessary costimulatory signal is provided by cluster of differentiation (CD) 80/CD86 and CD28 interaction. The polarization of the T-cell response is determined by the cytokine cocktail released by DCs during this DC/T-cell interaction.

1.2.1.3 Dendritic cells require activation

Generally, the loading of a suitable antigen onto major histocompatibility complex (MHC) molecules on DCs alone does not suffice to elicit an adaptive response (Martin et al. 2008). DCs must receive an additional activation stimulus (Figure 1, step 4). Activation initiates both a maturation process, required to attain full T-cell priming capability, and the migration process to the draining lymph node (Alvarez et al. 2008; Dalod et al. 2014).

For a long time, it has been unclear which skin-residing DC subset mediates sensitization. Recent studies suggest that each of the skin-residing DC subsets (Langerhans cells, cluster of differentiation (CD) 103^+ dermal DCs and $CD103^-$ dermal DCs) has the potential to prime T-cells in contact hypersensitivity and that the degree of involvement of the different subsets is highly contextual (Honda and Kabashima 2016; Honda et al. 2013).

1.2.1.4 Hapten-induced innate inflammation drives dendritic cell activation

Contact allergens activate DCs through pattern recognition receptors (PRRs), such as the $P2X_7$ purinergic receptor, receptors of the nucleotide-binding oligomerization domain-like receptor family and the Toll-like receptor (TLR) family among others (Martin et al. 2008; Esser et al. 2012; Weber et al. 2010). With the exception of nickel and cobalt, which are direct ligands for human TLR4 (Schmidt et al. 2010; Raghavan et al. 2012), contact allergens generally activate PPRs indirectly through danger-associated molecular patterns (DAMPs). DAMPs are endogenous PPR ligands associated with tissue damage, such as adenosine triphosphate (ATP), deoxyribonucleic acid (DNA), high mobility group box 1, formed in the skin upon exposure to the contact allergen (Figure 1, step 3) (Schaefer 2014).

Engagement of PPRs activates DCs both directly and indirectly, through the activation of other skin resident innate immune cells, which release proinflammatory cytokines, that in turn contribute to DC activation (Figure 1, step 5) (Honda et al. 2013). This ability of contact allergens to induce innate inflammation and create a proinflammatory milieu is described with the term "irritancy" and refers to a critical link between innate and adaptive immunity. The strength of the initial irritancy and therefore the initial inflammation facilitates DC activation and thus the entire adaptive immune response (Bonneville et al. 2007; Grabbe et al. 1996; Lass et al. 2010). The mechanisms of how contact allergens generate DAMPs are characteristic for each contact allergen. For example, oxazolone (OXA) causes ATP release in the exposed skin, thus activating DCs through the $P2X_7$ receptor and downstream inflammasome activation (Weber et al. 2010). Inflammasome activation is a common denominator of PRR signaling and crucial for the induction of CHS (Watanabe et al. 2008; Sutterwala et al. 2006). Inflammasome assembly facilitates the release of interleukin (IL)-18 and IL-1β. These cytokines are thought to be the main inflammatory cytokines driving DC activation (Antonopoulos et al. 2001; Antonopoulos et al. 2008; Shornick et al. 1996). Tumor necrosis factor (TNF) α is another crucial cytokine secreted by keratinocytes (Cumberbatch et al. 1997; Cumberbatch et al. 1999; Cumberbatch and Kimber 1995). Mast cells degranulate upon contact allergen exposure releasing histamine in the process, causing dilatation and increased permeability of skin vessels (Figure 1, step 6) (Dudeck et al.

2011). Neutrophil recruitment to the exposed skin, another requirement for successful sensitization, also depends on mast cells (Figure 1, step 7) (Weber et al. 2015).

1.2.1.5 Activated dendritic cells prime naïve T-cells in the draining lymph node

DC activation initiates both a maturation process and at the same time the emigration from the skin to the draining lymph node (Figure 1, step 8) (Alvarez et al. 2008). The maturation process entails the upregulation of co-stimulatory surface molecules required for full T-cell priming capability, such as CD80, CD86 and MHC II (Dalod et al. 2014). The mechanisms of DC emigration from the skin to the draining lymph node are a complex topic nicely reviewed by Alvarez et al. (Alvarez et al. 2008).

Upon arrival in the lymph node, DCs encounter naïve T-cells in the paracortical area of the lymph node (Figure 1, step 9). The priming of these naïve T-cells requires three signals (Peiser 2013). The first signal is provided by the interaction between TCR and the antigen loaded MHC molecule. The second signal is provided by the interaction of the co-stimulatory molecules CD86 and CD80 with CD28 (Kondo et al. 1996; Reiser and Schneeberger 1996). The third signal is provided by the cytokines released by DCs during T-cell/DC interaction. The composition of the cytokine cocktail determines the T-cell polarization (Walsh and Mills 2013). While the factors determining the cytokine cocktail are largely unclear, there is evidence that the cytokine environment in the skin is relevant here (Walsh and Mills 2013).

1.2.2 Effector phase

1.2.2.1 Innate activation precedes and shapes the antigen specific T-cell response

The predominant concept is that the effector phase is initiated by an antigen-independent activation of the innate branch of the immune system triggered through the "irritancy" of the respective contact allergen (Figure 2) (Honda et al. 2013). This initial innate inflammation promotes the subsequent influx of antigen specific T-cells which as the main effector cells convey the bulk of the skin inflammation (Honda et al. 2013).

Many of the mechanisms behind the initial innate inflammation in the sensitization phase also apply during the effector phase. DAMP formation and subsequent activation of innate immune cells through PPR engagement is again an important step (Figure 2, step 1) (Honda et al. 2013). For example, ATP again stimulates keratinocytes to secrete TNFα and IL-1β through the acti-

vation of $P2X_7$ (Watanabe et al. 2007; Sutterwala et al. 2006). Mast cells again degranulate, releasing histamine in the process, which induces dilatation and increased permeability of skin vessel and thus promotes neutrophil recruitment (Dudeck et al. 2011). Additionally, mast cells release TNFα and the neutrophil attracting chemokine (C-X-C motif) ligand 2 (CXCL2) (Biedermann et al. 2000). TNFα and IL-1β stimulate keratinocytes to further release an array of neutrophil and T-cell attracting chemokines (Sebastiani et al. 2002; Homey et al. 2002; Tohyama et al. 2001). Furthermore, TNFα and IL-1β stimulate endothelial cells to upregulate surface molecules required for leukocyte extravasation (Figure 2, step 3) (Kish et al. 2011; McHale et al. 1999; Harari et al. 1999). The chemokines work together with the endothelial activation to first recruit neutrophils and afterwards T-cells (Figure 2, step 4). Interestingly, the initial neutrophil recruitment was found to control the subsequent T-cell recruitment (Figure 2, step 5) (Engeman et al. 2004; Weber et al. 2015).

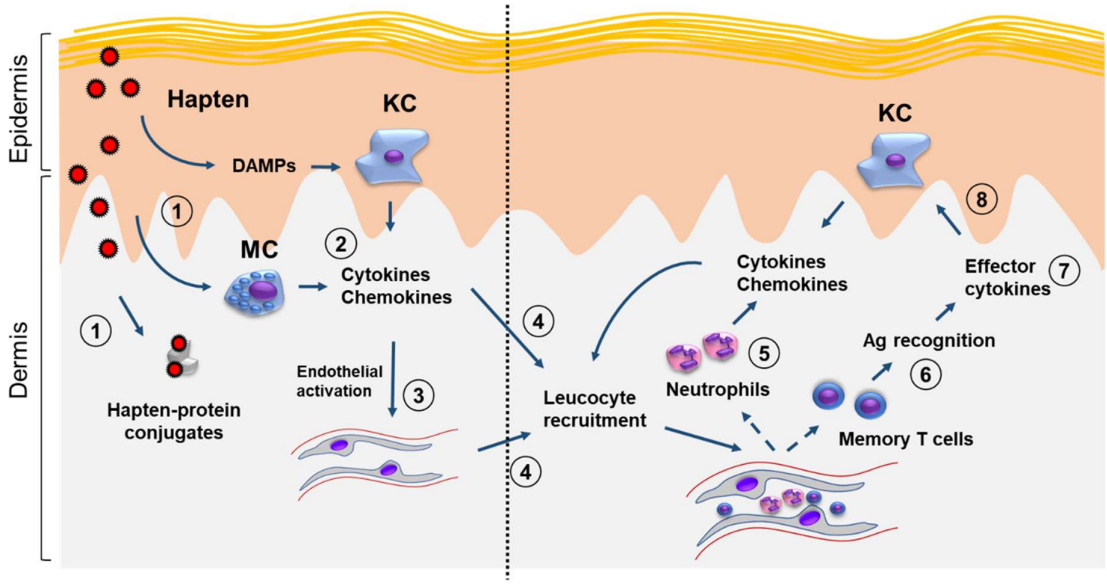

Figure 2: Innate and adaptive inflammation during the effector phase
Analogous to the sensitization phase, the effector phase starts off with activation of skin resident innate immune cells through danger-associated molecular patterns (DAMPs) and direct hapten effects (1). Keratinocytes (KCs) and mast cells (MCs) release a plethora of proinflammatory cytokines and chemokines (2). Among these are interleukin (IL)-1β and tumor necrosis factor (TNF) α, which activate endothelial cells to upregulate surface molecules required for leucocyte extravasation (3). The endothelial activation in conjunction with the chemokines facilitates recruitment of neutrophils and T-cells (4). An initial wave of neutrophils adds to the proinflammatory milieu (5) creating a positive feedback loop that is crucial for the subsequent T-cell recruitment. Recruited T memory cells recognize their cognate antigen (Ag) (6), releasing effector cytokines in the process (7), which in turn further activate keratinocytes (8).

It has been discovered recently that dendritic cells do not only play a pivotal role during sensitization, but also during the effector phase (Egawa et al. 2011). IL-1α released by keratinocytes

induces the formation of so called "perivascular leucocyte cell clusters" in the hapten-exposed dermis (Honda and Kabashima 2016; Egawa et al. 2011; Natsuaki et al. 2014). M2 macrophages located around postcapillary venules respond to IL-1α stimulation with CXCL2 release, which attracts dermal dendritic cells (Natsuaki et al. 2014). The accumulated dermal DCs present antigens to newly recruited T effector cells, allowing for local activation and proliferation of T-cells (Natsuaki et al. 2014).

It should be noted that there is evidence for an alternative concept, in which antigen specific T-cell recruitment and activation precede the neutrophil influx (Kish et al. 2011; Kish et al. 2009). Moreover, there is evidence for an involvement of B-cells and the complement system in the initial inflammation (Campos et al. 2003; Campos et al. 2006; Tsuji et al. 2002).

1.2.2.2 $CD8^+$ T-cells are the main effector cells

For years there had been a debate about the nature of the effector T-cell in CHS due to conflicting experimental findings. Depletion of $CD4^+$ cells was found to cause an exacerbated CHS response, whereas depletion of $CD8^+$ cells abrogated the CHS response (Xu et al. 1996; Gocinski and Tigelaar 1990; Bour et al. 1995). Mice that were depleted of both $CD8^+$ and $CD4^+$ cells display a diminished CHS response compared to the sole depletion of $CD8^+$ cells, suggesting a partial effector function for $CD4^+$ cells (Gocinski and Tigelaar 1990). Due to discovery of $CD4^+$ regulatory T-cells, it has become clear that $CD4^+$ cells comprise both anti-inflammatory regulatory cells as well as proinflammatory T helper cells. The current concept is that $CD8^+$ T-cell are the main effector cell type for most contact allergens and that in some cases $CD4^+$ helper cells may exhibit effector functions (Vocanson et al. 2009).

The polarization of these $CD8^+$ cytotoxic T-cells (Tc) is highly variable and depends on many factors, such as the genetic background of the mouse strain and the contact allergen used (Honda et al. 2013). Tc1, Tc2 and Tc17 cells can all fulfill the effector role (Vocanson et al. 2009). Tc1 cells, however, are considered the most important. Upon recognition of their cognate antigen Tc1 cells release their signature cytokines interferon γ and TNFα, which in turn stimulate keratinocytes and mast cells to release another wave of chemokines and proinflammatory cytokines (Figure 2, step 6-8) (Vocanson et al. 2009). This secondary wave provides a feedback loop augmenting the inflammation and recruiting more T-cells and neutrophils (Honda et al. 2013). Another key factor is the direct damage to keratinocytes (Kehren et al. 1999). Cytotoxic T-cells induce apoptosis of keratinocytes through the Fas/Fas ligand pathway (Akiba et al. 2002; Traidl et al. 2000; Trautmann et al. 2000).

1.3 Regulatory T-cells

Regulatory T-cells (Tregs or Treg cells) maintain self-tolerance and regulate immune responses (Sakaguchi et al. 2010). They are crucial for keeping autoimmunity in check as highlighted by the occurrence of a fatal autoimmune disease in Treg deficient humans and mice (Bennett et al. 2001; Brunkow et al. 2001). Numerous Treg cells have been identified, however, $CD4^+$ Tregs are considered to be the main regulators of peripheral immune responses. CD25, the α chain of the high affinity IL-2 receptor, is constitutively expressed by the majority of $CD4^+$ Tregs (~90%) and is widely used as a marker (Sakaguchi et al. 1995). Forkhead Box P3 (FoxP3) has been identified as the master transcription factor controlling Treg development, maintenance and function (Fontenot et al. 2003; Hori et al. 2003).

The mechanisms of how Tregs control immune responses can be classified into four modes of action (Figure 3) (Vignali et al. 2008). First, Tregs can disrupt T-cell responses through interfering with DC/T-cell interaction in a cell contact dependent fashion (Figure 3A). For example, cytotoxic T lymphocyte-associated protein 4 (CTLA-4) expressed by Tregs has a higher affinity towards CD80/CD86 compared to CD28, thus outcompeting CD28 in binding to the shared ligand (Walunas et al. 1994). The lack of CD28 signaling during TCR/MHC interaction renders T-cells anergic (Harding et al. 1992). Similarly, lymphocyte activation gene 3 (LAG-3) binds MHC II with a higher affinity than CD4 preventing T-cells from recognizing their MHC II bound cognate antigen (Andrews et al. 2017). Another mode of action is the secretion of inhibitory cytokines by Tregs, mainly IL-10 and transforming growth factor (TGF) β (Figure 3B) (Vignali et al. 2008). In particular IL-10 has broad anti-inflammatory effects on various immune cells, e.g. effector T-cells and antigen presenting cells (Moore et al. 2001). Importantly, these soluble factors allow Tregs to control immune responses without the need for co-localization of Tregs and the target cells. In a process termed "metabolic disruption" Tregs can clear proinflammatory molecules, such as ATP and IL-2 (Vignali et al. 2008). Specifically, Tregs degrade ATP to the anti-inflammatory adenosine through the ectonucleotidases CD39 and CD73 (Deaglio et al. 2007). Through their high affinity IL-2 receptor Tregs consume IL-2, which is a required proliferation stimulus for $CD8^+$ T-cells (Chinen et al. 2016). Lastly, Tregs control a T-cell response by lyzing effector T-cells through the granzyme pathway (Figure 3D) (Gondek et al. 2005). The exact contribution of each mode of action to the regulatory function of Tregs is specific to the context.

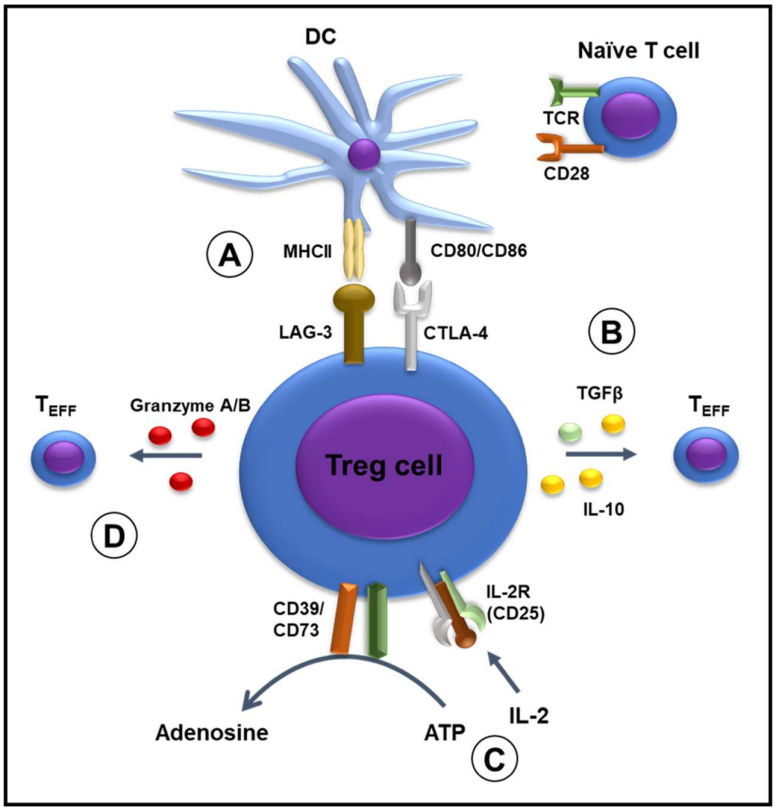

Figure 3: Mechanisms of Treg-mediated suppression
Regulatory T-cells (Treg cells) can disrupt the interaction between T-cells and dendritic cells (DCs) during T-cell priming in a cell contact dependent manner. Cytotoxic T-lymphocyte-associated protein (CTLA) 4 and lymphocyte activation gene (LAG) 3 expressed by Tregs bind cluster of differentiation (CD) 80/CD86 and major histocompatibility complex (MHC) II with a higher affinity than their T-cell counterparts, CD28 and CD4 (A). Tregs release inhibitory cytokines, mainly interleukin (IL)-10 and transforming growth factor (TGF) β (B). In a process termed "metabolic disruption" Tregs clear proinflammatory molecules (C). The high affinity IL-2 receptor on Tregs consumes IL-2 depriving T effector cells (T_{EFF}) of a proliferation stimulus. The ectonucleotidases CD39 and CD73 degrade the proinflammatory adenosine triphosphate (ATP) to the immunosuppressive adenosine. Tregs lyze T effector cells directly through the granzyme pathway (D).

1.3.1 Regulation of the sensitization phase by Tregs

The importance of $CD4^+$ $CD25^+$ $FoxP3^+$ regulatory T-cells for the regulation of both sensitization and effector phase in ACD have been shown in many studies (Kish et al. 2005; Tomura et al. 2010; Honda et al. 2011; Vocanson et al. 2006; Ring et al. 2006; Ring et al. 2010b). During the sensitization phase, the regulatory function of Tregs phase depends on Treg presence in the skin-draining lymph node. Impaired Treg homing to the draining lymph node due to CD62L deficiency abrogated any suppressive effect (Ring et al. 2010b). The exposure to the contact allergen during sensitization causes ATP release in the respective draining lymph nodes (Ring et al. 2010a; Mahnke et al. 2017). ATP activates Tregs through their purinergic receptors and simultaneously provides the substrate for the ectonucleotidases CD39 and CD73 (Ring et al.

2010b; Ring et al. 2010a). CD39 and CD73 are constitutively expressed on the surface of Tregs and are further upregulated upon activation (Ring et al. 2009; Deaglio et al. 2007). Together, they facilitate the degradation of ATP to adenosine (Deaglio et al. 2007). The activated Tregs form gap junctions with DCs, which facilitates the downregulation of CD86 and thereby disrupts T-cell priming (Ring et al. 2010b). At the same time, the Treg derived adenosine directs DC migration towards Tregs, further promoting DC/Treg interaction (Ring et al. 2015). Moreover, through ATP degradation Tregs interfere with the emigration of T-cells from the lymph nodes (Mahnke et al. 2017). Normally, ATP released upon sensitization binds to $P2X_7$ purinergic receptors on T-cells activating a disintegrin and metalloproteinase (ADAM) with a thrombospondin type 1 motif, member 13, which sheds CD62L from T-cell surfaces and thus enables their egress from the lymph node. The degradation of ATP through CD39 and CD73 prevents the necessary CD62L shedding (Mahnke et al. 2017).

1.3.2 Regulation of the effector phase by Tregs

In the effector phase, Tregs attenuate the ear-swelling response in mice by blocking the recruitment of leucocytes to the challenged skin (Ring et al. 2006). This is primarily achieved through the secretion of IL-10 and again adenosine (Ring et al. 2006; Ring et al. 2009). The presence of Tregs in the challenged skin is obsolete (Ring et al. 2009). The reapplication of the contact allergen during the challenge phase induces ATP release in the skin and in the blood (Ring et al. 2010a). As is the case in the sensitization phase, ATP activates Tregs and simultaneously provides the substrate for CD39 and CD73. The resulting adenosine downregulates E- and P-selectin on endothelial cells, thereby inhibiting leucocyte extravasation (Ring et al. 2009). Furthermore, Tregs have been shown to constantly circulate between the skin and the skin-draining lymph nodes both in the steady-state and under inflammatory conditions (Egawa et al. 2011). Tregs that migrated from challenged skin to the lymph node display an activated effector/memory phenotype with high expression levels of CD25, CD103, CD44, CD69 and show particularly strong immunosuppressive activity *in vitro* and *in vivo* (Egawa et al. 2011). These migratory Tregs retain the ability to reenter the skin (Egawa et al. 2011). However, their contribution towards the regulation of the effector phase is unclear.

1.4 The α_E(CD103)β_7 integrin

1.4.1 Structure and distribution of α_E(CD103)β_7 integrin

CD103 is the designation of the α_E subunit of the heterodimeric integrin α_E(CD103)β_7 (Figure 4) (Micklem et al. 1991). While the β_7 chain can also pair with α_4 (CD49d), forming the α_4(CD49d)β_7 integrin, α_E(CD103) exclusively heterodimerizes with β_7. CD103 is often used to refer to the entire integrin α_E(CD103)β_7.

CD103 shows a restricted expression pattern on immune cells in both mice and humans. Major CD103 expressing cell populations include innate-lymphoid cells (ILC), DCs, Tregs, tissue-resident memory T-cells, cytotoxic T-cells and mast cells (Hardenberg et al. 2018). The only identified ligand to this day is E-cadherin (Cepek et al. 1994; Karecla et al. 1995; Higgins et al. 1998), though there is strong evidence of another yet unidentified ligand (Brown et al. 1999; Strauch et al. 2001; Jenkinson et al. 2011).

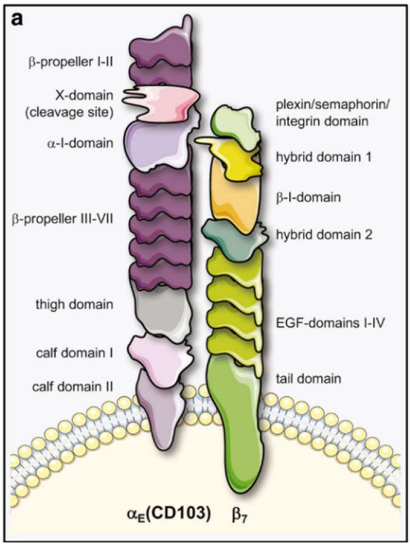

Figure 4: Domain structure of the α_E(CD103)β_7 integrin
Domain structure of the α_E(CD103)β_7 integrin. The propeller, calf, and thigh domains of the α_E(CD103) chain are shared with all known integrin α-subunits, whereas the α-I-domain is found in eight others. The X-domain containing a proteolytic cleavage site is unique to α_E(CD103). From Hardenberg et al. 2018.

The function of CD103 has been studied most extensively in T lymphocytes. For a long time, the main function of CD103 was assumed to be the retention of T-cells within epithelial compartments (Pauls et al. 2001; Schlickum et al. 2008). Recently, however, a major role of CD103 in tumor immunity has emerged. CD103 does not only facilitate the retention of $CD8^+$ cytotoxic

T-cells to tumor tissue, it also contributes directly to the lysis of these tumor cells (Corgnac et al. 2018; Duhen et al. 2018). In fact, CD103 expression by tumor infiltrating $CD8^+$ cytotoxic T-cells is a predictive marker for favorable prognosis in several neoplasms (Duhen et al. 2018). Murine dermal ILC2s uniformly express CD103 (Roediger et al. 2013). However, nothing is known about the exact function of CD103 for these cells yet. While CD103 is an important marker for several murine dendritic cell subsets in different tissues (del Rio et al. 2010), its function on dendritic cells is not clear yet.

1.4.2 CD103 expressing regulatory T-cells

CD103 marks a distinct Treg subset throughout several tissues. About 90% of dermal Tregs, about 25% of lymphoid Tregs and about 80% of Tregs in the lamina propria of the small intestine express CD103 (Yuan et al. 2015; Braun et al. 2015; Lehmann et al. 2002; Suffia et al. 2005; Banz et al. 2003). However, only one study so far has shown a direct relevance of CD103 for Treg function (Belkaid et al. 2002). The dermal retention of $CD4^+$ Tregs in a model of cutaneous leishmaniasis was found to be mediated by CD103 (Suffia et al. 2005). These $CD103^+$ Tregs suppressed the immune response enabling the persistence of the pathogens in the skin. Analysis of activation markers show that $CD103^+$ Tregs display an activated effector/memory phenotype, as demonstrated by increased levels of CTLA-4, inducible T-cell co-stimulator, CD44, glucocorticoid-induced TNF-receptor-related protein, CD69, granzyme B, Fas ligand, C-C chemokine receptor (CCR) 3, and CCR5 (Chang et al. 2012; Lin et al. 2009; Siewert et al. 2008). A number of studies revealed the CD103 expressing subset to have greater immunosuppressive potential *in vivo* (Lehmann et al. 2002; Banz et al. 2003; Chang et al. 2012; Hühn et al. 2004). Furthermore, $CD103^+$ Tregs feature higher FoxP3 expression levels, however, no causal relation between CD103 expression and FoxP3 expression has been discerned (Braun et al. 2015; Lehmann et al. 2002; Hühn et al. 2004). In several murine cancer models tumor infiltrating Tregs express CD103, however, it was found to be dispensable for Treg retention in the tumor and is thought to be a byproduct of a microenvironment rich in TGFβ (Anz et al. 2011).

CD103 expression by Tregs is primarily controlled by TGFβ. Selective deletion of the TGFβ receptor 1 in $FoxP3^+$ Tregs led to a heavily diminished CD103 expression on these cells throughout the body (Konkel et al. 2017). This TGFβ responsiveness of the integrin α_E(CD103) gene is conveyed through a SMAD3 binding promotor site and through additional SMAD3 enhancer elements (Mokrani et al. 2014; Robinson et al. 2001). TCR signaling can also induce CD103 expression through a nuclear factor of activated T-cells enhancer element. (Mokrani et al. 2014)

1.5 The role of CD103 in allergic contact dermatitis

Evidence for a role of CD103 in inflammatory skin disease was first observed in the late 90s, when newly generated CD103 knockout ($CD103^{-/-}$) mice developed spontaneous inflammatory skin lesions (Schön et al. 2000). This prompted the idea that CD103 might be relevant for inflammatory skin diseases in general.

Indeed, when CHS responses of $CD103^{-/-}$ mice (backcrossed on a C57BL/6J genetic background) towards OXA and dinitrochlorobenzene were investigated the ear-swelling response was increased (Braun et al. 2015). CD103 expressing cells relevant in the pathophysiology of CHS include dermal $Langerin^+$ DCs, $CD8^+$ cytotoxic T-cells, $CD4^+$ $CD25^+$ regulatory T-cells, and dermal ILC2. CD103 deficiency on either of these cells could have been responsible for the aggravated CHS response.

Investigation of DC function in $CD103^{-/-}$ mice during the sensitization phase yielded no discernable abnormalities (Braun et al. 2015). Langerhans cell morphology and *in situ* cell counts and distribution were normal, as was the number of antigen-loaded DCs that migrated to the skin-draining lymph nodes following fluorescein isothiocyanate painting. DCs showed similar expression levels of common activation markers and *in vitro* analysis using bone marrow-derived DCs showed unaltered T-cell activating capacity. A possible role of CD103 for DC function in the effector phase was not investigated, however.

The elevated CHS response could be transferred to wildtype (wt) mice and even to $Rag1^{-/-}$ mice in adoptive transfer experiments using draining lymph node (dLN) cell suspensions from sensitized $CD103^{-/-}$ mice (Braun et al. 2015). Since T-cells make up the bulk of dLN cells, this strongly suggested T-cells as the mediators of the aggravated CHS response. Indeed, *in vivo* primed $CD8^+$ T-cells from $CD103^{-/-}$ mice proliferated more strongly upon *in vitro* re-exposure to the contact allergen, indicating a dysregulation of T-cell proliferation (Braun et al. 2015). This could be caused either directly by the intrinsic deficiency of CD103 on $CD8^+$ T-cells and/or by a disruption of regulatory mechanisms during sensitization and/or effector phase.

Hence, $CD4^+$ $CD25^+$ T-cells, the main regulators of CHS, stepped into the spotlight. Indeed, preliminary investigations yielded evidence for altered Treg function in $CD103^{-/-}$ mice. Flow cytometric analysis of dermal Tregs in the effector phase found the FoxP3 expression of Tregs in $CD103^{-/-}$ mice to be diminished (Braun et al. 2015). The same analysis in the steady-state yielded no differences, thus hinting at a role of CD103 in the upregulation of FoxP3 after activation.

1.6 Aim of this thesis

The aim of this study was to further elucidate the role of CD103 for Treg function in CHS. More concretely this thesis aimed to answer the following questions:

1. Are Tregs in CD103$^{-/-}$ mice impaired in their regulatory function during the sensitization phase and/or effector phase?
2. Is CD103 involved in intradermal retention of T-cells?
3. Is the upregulation of FoxP3 after Treg activation dependent on CD103? Are Tregs in CD103$^{-/-}$ mice impaired in their ability to be activated?

In a first experiment, it was investigated whether Tregs in CD103$^{-/-}$ mice are equally capable of suppressing sensitization compared to Tregs in wt mice. For that purpose, Tregs were isolated from wt mice (wt Tregs) and CD103$^{-/-}$ mice (CD103$^{-/-}$ Tregs) and injected intravenously into groups of naïve wt mice. Sensitization was performed the next day, and CHS was elicited on the right ears after 5 more days. The ear-swelling measured over a 96-hour timespan served as the readout parameter.

Next, the ability of CD103$^{-/-}$ Tregs to suppress the effector phase was examined, again compared to wt Tregs. Rag-1$^{-/-}$ mice were injected either with wt Tregs or CD103$^{-/-}$ Tregs prior to elicitation of the effector phase. The impact on the resulting ear-swelling response was studied. Since Rag-1$^{-/-}$ mice are devoid of endogenous mature lymphocytes, using these mice allowed the selective analysis of donor cells. These mice were reconstituted with draining lymph node cells parallel to Treg transfers and CHS was subsequently induced.

To study the role of CD103 for the dermal retention of T-cells, CD103 competent and CD103 deficient lymphocytes were injected intradermally into the ears of mice and their presence was tracked over time by flow cytometry.

Last, to answer whether Tregs in CD103$^{-/-}$ mice are impaired in the ability to be activated and to upregulate FoxP3, CD103$^{-/-}$ mice and wt mice were treated with the super agonistic CD28 antibody (aCD28SA), clone D665. This antibody is a potent and preferential activator of Treg cells (Gogishvili et al. 2009). The effect of aCD28SA on Tregs was assessed in the lymph nodes through analyzing the frequency of CD4$^+$ CD25$^+$ FoxP3$^+$ cells and the expression levels of CD25 and FoxP3.

2 Material

2.1 Animals

An overview of the mouse strains used in this thesis is provided in Table 1. Mice were housed in the animal care facility of the University of Göttingen. All mice were held in individually ventilated cages with a 12 h light/dark cycle and unrestricted access to food and water. Only mice between the age of 8 and 12 weeks were used in experiments. The experiments were performed in accordance with the institutional, state and federal guidelines and were approved by local institutional animal care advisory committees and the respective permit authorities (Tierversuchsantrag 15/1789).

Table 1: Mouse strains used in experimental procedures

Animals	Origin
C57BL/6	Charles River, Germany
$CD103^{-/-}$	(Schön et al. 1999)
DEREG	(Lahl et al. 2007)
$Rag\text{-}1^{-/-}$	Charles River, Germany

2.2 Chemicals, solutions, buffers and media

Table 2: Chemicals

Chemical	Manufacturer
Acetone	Th. Geyer GmbH & Co. KG, Renningen, Germany
β-Mercaptoethanol	Carl Roth GmbH + Co. KG, Karlsruhe, Germany
Carboxyfluorescein succinimidyl ester (CFSE)	Sigma-Aldrich Corporation, Munich, Germany
Dimethylsulfoxid (DMSO)	Carl Roth GmbH + Co. KG
Ethanol absolut	Carl Roth GmbH + Co. KG
Ethylenediaminetetraacetic acid (EDTA)	Thermo Fisher Scientific, Dreieich, Germany
Glutamin	Fisher Scientific GmbH, Schwerte, Germany
Hydroxyethylpiperazineethanesulfonic acid (HEPES)	Thermo Fisher Scientific
Isoflurane	AbbVie GmbH & Co. KG, Ludwigshafen, Germany
Oxazolone	Sigma-Aldrich Corporation
Sodium pyruvate	Thermo Fisher Scientific
Trypan blue	Sigma-Aldrich Corporation

Table 3: Solutions, buffers and media

Solution	Recipe	Manufacturer
Ear digestion enzyme coctail	66% Liberase	Hoffmann-La Roche (Roche), Basel, Switzerland
	10% DNAse	Hoffmann-La Roche (Roche)
		AppliChem GmbH, Darmstadt, Germany
	24% RPMI 1640	Lonza Group, Basel, Switzerland
FACS cleaning solution		Becton Dickinson GmbH, Heidelberg, Germany
FACS sheath fluid		Becton Dickinson GmbH
FACS shutdown solution		Becton Dickinson GmbH
FoxP3 Fix/Perm buffer Set		BioLegend GmbH, Koblenz, Germany
MACS buffer	PBS	Lonza Group, Basel, Switzerland
	2-mM EDTA	Thermo Fisher Scientific
	0.5% FCS	Biochrom GmbH, Berlin, Germany
RPMI complete medium	RPMI 1640	Lonza Group
	10% FCS	Biochrom GmbH
	2 mM Glutamin	Fisher Scientific GmbH
	100 U/ml Penicillin	Fisher Scientific GmbH
	100 µg/ml Streptomycin	Fisher Scientific GmbH
	50 µM β-Mercaptoethanol	Carl Roth GmbH + Co. KG
	25 mM HEPES	Thermo Fisher Scientific
	1.1 mM Sodium pyruvate	Thermo Fisher Scientific
	0.1 mM Non-Essential Amino Acids (NEAA)	Thermo Fisher Scientific

2.3 Kits

Table 4: Kits

Kits	Manufacturer
$CD4^+CD25^+$ Regulatory T-cell Isolation Kit, Mouse	Miltenyi Biotec GmbH, Bergisch Gladbach, Germany
CellTrace™ Far Red Cell Proliferation Kit	Thermo Fisher Scientific
Zombie NIR™ Fixable Viability Kit	BioLegend GmbH

2.4 Antibodies and toxins used for *in vivo* use

Table 5: Biochemicals used in animal experiments

Name	Clone	Manufacturer
Diphtheria toxin		Sigma-Aldrich Corporation
Mouse CD28 antibody	D665	Bio-Rad AbD Serotec GmbH, Puchheim, Germany

2.5 Antibodies used in flow cytometry

Table 6: Mouse antibodies

Antigen	Conjugate	Clone	Volume per 10^6 cells	End concentration in [µg/ml]	Isotype	Manufacturer
CD4	Peridinin-Chlorophyll-protein (PerCP)	RM4-5	5 µl	0.1	Rat IgG2a, κ	Becton Dickinson GmbH
CD8	Phycoerythrin (PE)	53-6.7	0.05 µl	0.01	Rat IgG2a, κ	BioLegend GmbH
CD16/32		93	2 µl	0.1	Rat IgG2a, λ	BioLegend GmbH
CD25	Brilliant Violet 421™	PC61	0.5 µl	0.1	Rat IgG1, λ	BioLegend GmbH
CD103	Alexa Fluor® 488	2E7	5 µl	0.25	Armenian Hamster IgG	BioLegend GmbH
FoxP3	Alexa Fluor® 647	MF-14	2 µl	1	Rat IgG2b, κ	BioLegend GmbH
TCRβ chain	Brilliant Violet 510™	H57-597	5 µl	0.1	Armenian Hamster IgG	BioLegend GmbH

Table 7: Corresponding isotype control antibodies

Conjugate	Clone	Isotype	Manufacturer
PerCP	A95-1	Rat IgG2b, κ	Becton Dickinson GmbH
PE	TBE15	Rat IgG2b	ImmunoTools, Friesoythe, Germany
Brilliant Violet 421™	RTK2071	Rat IgG1, κ	BioLegend GmbH
Alexa Fluor® 488	HTK888	Ar Ham IgG	BioLegend GmbH
Alexa Fluor® 647	RTK2758	Rat IgG2a, κ	BioLegend GmbH
Brilliant Violet 510™	HTK888	Ar Ham IgG	BioLegend GmbH

2.6 Laboratory equipment and consumables

Table 8: Laboratory equipment

Equipment	Model	Manufacturer
Anesthesia system	VisualSonics VevoTM Compact Anesthesia System	VisualSonics, Toronto, Canada
Biosafety cabinet	LabGard® ES NU-540 Class II, Type A2 Biosafety Cabinet	NuAire, Plymouth, MN, USA
	Safe 2020 Class II Biological Safety Cabinets	Thermo Fisher Scientific
Camera	Fujifilm FinePix HS20 EXR	Fujifilm, Tokyo, Japan
Centrifuge	Heraeus Megafuge 1.0	Thermo Fisher Scientific
	Heraeus Megafuge 16R	Thermo Fisher Scientific
	Sprout Mini centrifuge	Biozym Scientific GmbH, Hessisch Oldendorf, Germany
CO_2 incubator	Heracell™ 150i CO_2 Incubator	Thermo Fisher Scientific
Drying chamber		Thermo Fisher Scientific
External measuring gauge	Kroeplin C220T	Kroeplin GmbH, Schlüchtern, Germany
Flow cytometer	BD FACSCanto II Flow Cytometer	Becton Dickinson GmbH
Freezer -20°C		Liebherr-International GmbH, Biberach an der Riß, Germany
Freezer -80°C	Sanyo Biomedical Freezer	Panasonic Corp., Kadoma, Japan
Fridge 4°C		Liebherr-International GmbH
Hair clipper	Panasonic ER-1411 Hair Clipper	Panasonic Corp.
Counting chamber	Neubauer Improved	Laboroptik Ltd, Lancing, UK
Inverse microscope	Axiovert 40C	Carl Zeiss, Göttingen, Germany
Laboratory water bath		Memmert GmbH + Co. KG, Schwabach, Germany
MACS MultiStand	MACS MultiStand	Miltenyi Biotec GmbH
MidiMACS™ Separator		Miltenyi Biotec GmbH
MiniMACS™ Separator		Miltenyi Biotec GmbH
Pipettor	PIPPETBOY acu	Integra Biosciences GmbH, Biebertal, Germany
Precision scale	AccuLab ALC-210.4	Sartorius, Göttingen, Germany
Pipettes	Eppendorf Research® plus (100-1000 µl)	Eppendorf AG, Hamburg, Germany
	Transferpette® S (2-200 µl)	Brand GmbH, Wertheim, Germany
	Eppendorf Research® plus (0.5-10 µl)	Eppendorf AG
Ultrasonic bath	Bandelin SONOREX™ RK100 Ultrasonic bath	Bandelin electronic GmbH & Co. KG, Berlin, Germany
Vortex mixer	Vortex-Genie 2	Scientific Industries, Inc., Bohemia, New York, USA

Table 9: Consumables

Consumable	Type	Manufacturer
Cannula	Sterican® Insulin G 30	B. Braun Melsungen AG, Melsungen, Germany
Centrifuge tubes	CELLSTAR® Centrifuge Tubes 15, 50 ml	Greiner Bio-One GmbH, Frickenhausen, Germany
Coverslip		Thermo Fisher Scientific
Culture plates	24 Well Cell Culture Multi-well Plate	Greiner Bio-One GmbH
	96 Well Polystyrene Cell Cultur microplate	Greiner Bio-One GmbH
FACS tubes	5 ml Round Bottom Polystyrene Test Tube	Becton Dickinson GmbH
Gloves	Gentle Skin® sensitive	Meditrade GmbH, Kiefersfelden, Germany
Graduated tips	TipOne® Tips 10, 200, 1000 µl	STARLAB GmbH, Hamburg, Germany
MACS columns	LD columns	Miltenyi Biotec GmbH
	MS Columns	Miltenyi Biotec GmbH
Parafilm	PARAFILM® M	Bermis, Neenah, Wisconsin, USA
Reaction tubes	1.5, 2 ml	Sarstedt AG & Co., Nümbrecht, Deutschland
Serological pipettes	5, 10, 25 ml	Sarstedt AG & Co.
Strainers	Falcon® 70µm Cell Strainer	Becton Dickinson GmbH
	50 µm Filcon, Non-sterile, Cup-Type	Corning, Corning, New York, USA
Syringe	B Braun Omnifix Syringes 10 ml Sterile	B. Braun Melsungen AG
	Injekt®-F Solo	B. Braun Melsungen AG

2.7 Software

Table 10: Software

Software	Manufacturer
Adobe Photoshop CC 2017	Adobe, San Jose, CA, USA
BD FACSDiva Software Version 8.0.1	Becton Dickinson GmbH
Microsoft Office 2016	Microsoft, Redmont, USA
Prism 6 for Windows V. 6.07	GraphPad Software Inc., La Jolla, CA, USA

3 Methods

3.1 Mouse handling and anesthesia

All animal handling was carried out in a biosafety cabinet. Mice were anaesthetized prior to all experimental procedures, using an isoflurane vaporizer. The anaesthesia was performed as follows: Mice were transferred from their individually ventilated cages into an air tight box, which was then ventilated with a mixture of isoflurane and oxygen. For intravenous and intradermal injections mice were ventilated with a small snout mask, allowing for continuous anesthesia during these procedures. Retroorbital injection technique was used for intravenous injections (Yardeni et al. 2011). Mice were killed either through cervical dislocation or by CO_2 asphyxiation. CO_2 asphyxiation was preferred when draining lymph nodes of the neck area were to be harvested post mortem.

3.2 Contact hypersensitivity model

The CHS model is the murine equivalent of allergic contact dermatitis and is used to study the pathophysiology of ACD (Honda et al. 2013). If not otherwise stated, the following protocol (Figure 5) was used to induce and elicit contact hypersensitivity. One day prior to sensitization (d-1) the lower backs of mice were shaved with an electric hair clipper. On d0, sensitization was achieved by applying 3 μg OXA dissolved in 100 μl ethanol with a 200 μl pipette on the shaved area. The mice were kept under anaesthesia until the alcohol was completely evaporated.

The OXA solutions were generated as follows: A small amount of OXA was spooned into a 2ml reaction tube. The exact quantity was then determined with a precision scale. Next, an appropriate volume of 100% ethanol was added to reach the desired concentrations of 3 μg OXA (3% OXA) or 1 μg OXA (1% OXA), respectively, per 100 μl ethanol. For complete dissolution, the mixture was then placed into an ultrasound bath for 5 minutes. After 5 days (on d5), the effector phase was initiated by reapplying the contact allergen, a process termed "challenge": 20 μl of the 1% OXA solution was applied onto the right ear. The left ear was treated with 20 μl ethanol to provide a vehicle control. From challenge onwards, the ear thickness was measured using an electronic external caliper. Each ear was measured in a standardized way at three measuring points (anterior, medial and posterior), and the average thickness was calculated. The increase in ear-swelling was determined as the normalized difference between the

OXA-treated and the vehicle-treated ear of the same mouse. Data were collected at the following time points: 0 h, 8 h, 24 h, 32 h, 48 h, 56 h, 72 h, 96 h. Importantly, the 0 h values were measured prior to challenge.

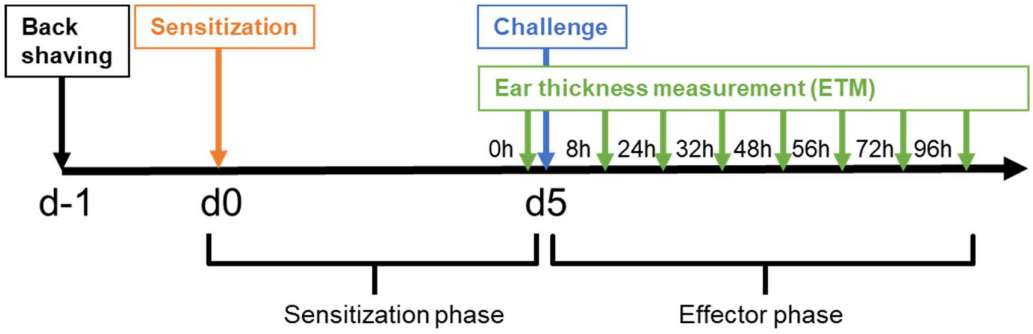

Figure 5: Contact hypersensitivity protocol

3.3 Preparation of single cell suspensions and Treg isolation

3.3.1 Ear tissue

For flow cytometry, skin cells must first be removed from their tissue and brought into a single cell suspension. Towards that end, donor mice were killed by CO_2 asphyxiation. The ears were then cut off at the base with scissors followed by removal of the remaining fur. Next, using two forceps, each ear was separated into two layers. The layers were put separately into wells of a 24 well plate. Each well had been filled beforehand with 500 µl of an enzyme cocktail (Table 3), which serves to break up the extracellular matrix as well as cell-cell contacts. Within these wells, the ear layers were cut into small pieces with scissors, and incubated at 37°C and 5% CO_2 for 90 min. Thereafter, the enzyme reaction was stopped through addition of 50 µl FCS to each well. The content of each well was further homogenized by agitating with a 500 µl pipette tip a hundred times per well. The cell suspensions were then strained through a 50 µm cell strainer. Both wells and cell strainer were rinsed twice with 500 µl PBS. The resulting suspension was centrifuged at 1300 rounds per minute (RPM) for 7 min. The pellet was resuspended in 1 ml PBS. Trypan blue-stained cells were counted using a Neubauer chamber.

3.3.2 Lymph node tissue preparation

Donor mice were killed by CO_2 asphyxiation. Mice were then pinned belly upwards on polystyrene. The belly was disinfected with 70% ethanol and the skin was cut from symphysis to chin using scissors. The skin was then peeled back, using forceps to reveal the skin-draining lymph

nodes. Lymph nodes were harvested from the inguinal, axillary and brachial, submental and cervical regions. Lymph nodes were collected in a 15 ml tube filled with sterile PBS and put on ice. Under a sterile bench a lymphocyte cell suspension was prepared by squashing the lymph nodes with a syringe plunger through a 70 µm strainer into a 50 ml tube, followed by repeated rinsing with sterile PBS. Afterwards, the suspension was centrifuged at 1300 RPM for 7 minutes. One ml of 0.5% DNAse (10% DNAse diluted to 0.5% with H_2O) was added to the pellet together with 4 ml of PBS. After mixing, the suspension was transferred into an CO_2 incubator for 5 minutes. After incubation, the cells were washed, centrifuged and counted as above.

3.3.3 Treg isolation by magnetic cell separation

Treg isolation was performed using the $CD4^+$ $CD25^+$ regulatory T-cell isolation kit according to the manufacturer's instructions. The kit is based on the principle of magnetic cell separation (MACS). A negative selection step, in which non-CD4 cells are magnetically labelled and depleted, is followed by a positive selection step, in which magnetically labelled $CD25^+$ cells are enriched. All centrifugation was done at 300 x g for 10 min in a cooled centrifuge (4°C). All incubation steps were done at 4°C and protected from light. The volumes for buffer and antibody solutions provided in this paragraph are indicated for 10^7 cells and were scaled upwards according to actual cell numbers. Antibody incubation was performed in 15 ml tubes. For washing cells, were transferred to 50 ml tubes. MACS buffer was generated as depicted in Table 3. Prior to use, the buffer was degassed by placing the tubes with partially opened lids into an ultrasound bath for 5 min. Aliquots of 10 µl were kept at all stages of the isolation process to later determine the purity through flowcytometry. Tregs from $CD103^{-/-}$ and wt mice were isolated simultaneously with two MiniMACS™ and MidiMACS™ separators.

The single cell suspension was centrifuged, followed by resuspension of the pellet in 40 µl buffer. 10 µl Biotin-Antibody-Cocktail was added and the mix was incubated for 10 minutes. Now, 30 µl buffer, 20 µl Anti-Biotin MicroBeads and 10 µl CD25-PE antibody were added, followed by incubation for 15 minutes. Afterwards cells were washed with 2 ml buffer. At the same time, the MACS Multistand was set up by placing a LD column in the appropriate MidiMACS™ separators. The LD column was rinsed with 2 ml buffer before the cell suspensions were applied. The centrifuged cells were resuspended in 90 µl buffer and then applied onto the column. The flow-through was collected in 15 ml tubes. The column was rinsed twice with 1 ml buffer. The flow-through was centrifuged and afterwards suspended in 90 µl buffer. 10 µl Anti-PE MicroBeads were added, followed by incubation for 15 minutes. Parallel to incubation the MS column was placed into the MiniMACS™ separator and rinsed with 500 µl buffer. The flow-

through of the first column was then applied onto the MS column. The column was rinsed two times with 500 µl buffer. After emptying of the reservoir, column was removed from the separator and placed onto a 15 ml tube. Next, 1 ml buffer was added, and the column was flushed using the plunger. This final effluent contained the purified $CD4^+$ $CD25^+$ Tregs. The number of vital Tregs was counted using trypan staining and a Neubauer counting chamber. Only Tregs with a purity >90% were used in experiments. For Treg adoptive transfer experiments the cells were washed one more time and resuspended at a concentration of $0.5*10^6$ Tregs per 150 µl PBS.

3.4 Treg depletion, recovery kinetics and CHS model in DEREG mice

To establish the efficacy and duration of Treg depletion, DEREG mice were injected intraperitoneally with freshly thawed 1 µg diphtheria toxin (DT) dissolved in 500 µl of PBS. After varying time intervals, the mice were killed, skin-draining lymph nodes harvested and Tregs analyzed by flow cytometry (see 3.7 for the staining protocol). All handling with DT toxin was performed under the required safety regulations. In order to test the impact of Treg depletion on the CHS response, the standard CHS protocol with the modified lag time of 12 days was carried out. Treg depletion was achieved through DT injection the day before sensitization (d-1). Using the same protocol, the standard concentrations of 3%/1% OXA for sensitization/challenge were compared with the lowered concentrations of 0.1%/1%.

3.5 Adoptive transfer experiments

3.5.1 Treg transfers prior to sensitization in wt mice

This protocol was designed to compare the suppressive effects of wt Tregs and $CD103^{-/-}$ Tregs on sensitization (Figure 6). Tregs were isolated from skin dLNs of naive wt C57BL/6 mice (wt Tregs) as well as $CD103^{-/-}$ mice ($CD103^{-/-}$ Tregs) (3.3.3). The freshly isolated Tregs were suspended separately in PBS at a concentration of $0.5*10^6$ per 150 µl PBS. A third tube filled with an equal volume of PBS and was used as a vehicle control. Naïve wt mice were then intravenously injected in three separate groups (retroorbital injection technique): One group received 150 µl of the vehicle, another group $0.5*10^6$ wt Tregs, and a third group $0.5*10^6$ $CD103^{-/-}$ Tregs.

A technician replaced the labels on the tubes containing the Treg cell suspensions and the vehicle control with a color marking, thus blinding the experimenter. The treatment regimen matching the chosen color was recorded, sealed in a letter and opened after the final ear-swelling

measurement. The backs of all treated mice were shaved on the same day. On the next day, mice were sensitized according to the standard CHS protocol (3.2).

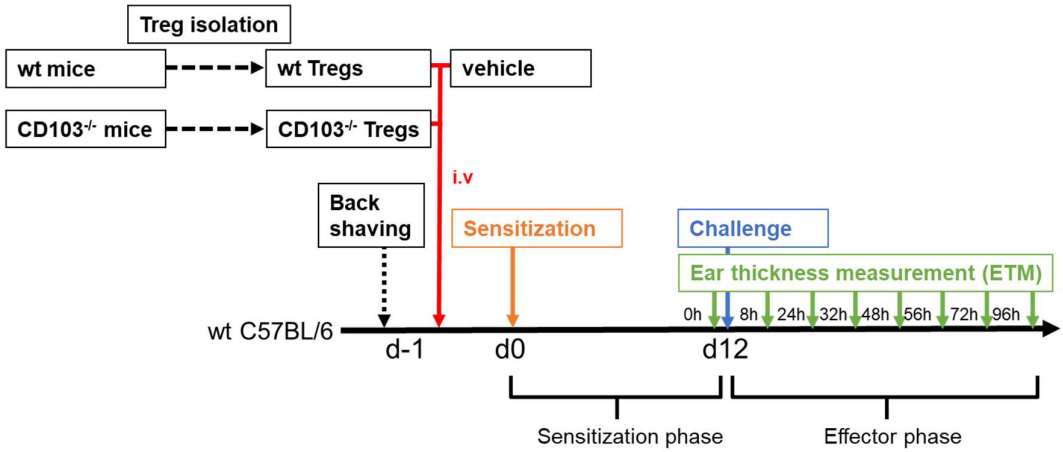

Figure 6: Treg transfer in wt mice prior to sensitization

3.5.2 Treg transfers prior to sensitization phase in DEREG Mice

It was first tested if Treg-depleted DEREG mice sufficed as recipients and showed a suppressive effect of adoptively transferred wt Tregs. DEREG mice were injected with either $1*10^6$ wt Tregs, $0.5*10^6$ wt Tregs or an equal volume of vehicle (PBS). DT was administered 2-4 hours prior to Treg transfers. The lower backs were shaved on the same day. Sensitization was carried out on the next day. The modified CHS with a 12-day lag time and the lowered OXA concentrations of 1%/0.1% for sensitization/challenge was performed. Treg isolation and injection were performed as described in 3.5. 1.

Since $0.5*10^5$ wt Tregs successfully suppressed sensitization (4.1.3), wt and $CD103^{-/-}$ Tregs were compared in an identical experimental setup. Treg-depleted DEREG mice were injected either with $0.5*10^6$ wt Tregs, $0.5*10^6$ $CD103^{-/-}$ Tregs or an equal volume of PBS (Figure 7).

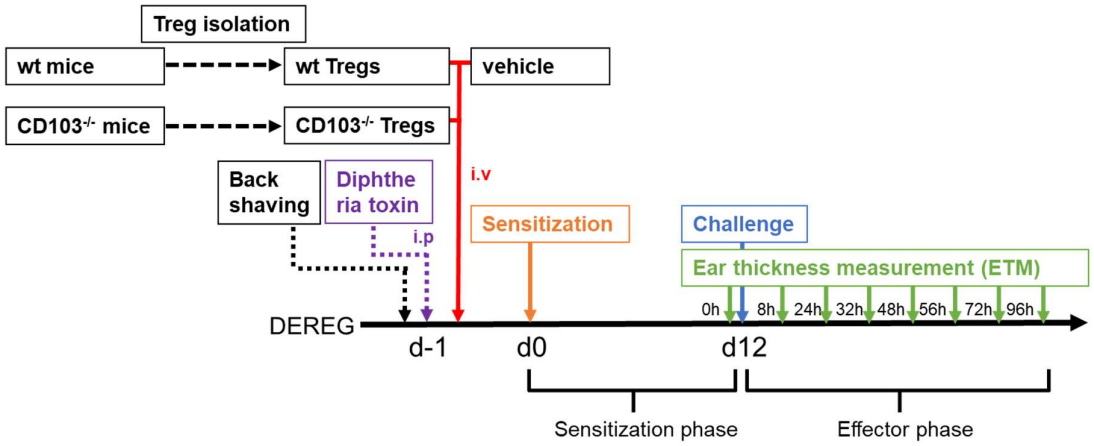

Figure 7: Treg transfer in Treg-depleted DEREG mice prior to sensitization

3.5.3 Treg transfer prior to effector phase in Rag-1$^{-/-}$ mice

This experiment was designed to compare the suppressive effect of transferred wt Tregs and CD103$^{-/-}$ Tregs on the effector phase. Reconstituted Rag-1$^{-/-}$ mice were chosen as recipients for adoptive transfers. Rag-1$^{-/-}$ mice lack functional endogenous lymphocytes (Mombaerts et al. 1992), thus precluding "intrinsic" T-cell biases. Rag-1$^{-/-}$ mice were reconstituted with draining lymph node cells from previously sensitized wt C57BL/6 mice (OXA dLN cells) and at the same time with either wt or CD103$^{-/-}$ Tregs (Figure 8). OXA dLN cell donor mice had their entire backs shaven, instead of only the lower back, and 200 µl of 3% OXA was applied for sensitization, instead of the usual 100 µl. This assured that all skin-draining lymph nodes removed (inguinal, axillary, brachial and cervical) contained OXA primed lymphocytes. The OXA dLN cells were harvested after 5 days. On the same day, Tregs were harvested from naive wt mice and CD103$^{-/-}$ mice. The isolated wt and CD103$^{-/-}$ Tregs cell were resuspended with the OXA dLN cells at a concentration of $2*10^7$ OXA dLN cells and $0.5*10^6$ Tregs per 150 µl PBS. This allowed reconstitution and Treg treatment to be performed in a single intravenous injection. A vehicle control with only $2*10^7$ OXA dLN cells in 150 µl PBS was also prepared.

Groups of Rag-1$^{-/-}$ mice were treated as follows: Group 1 was treated with $2*10^7$ OXA dLN cells. Group 2 was treated with $0.5*10^6$ wt Tregs and with $2*10^7$ OXA dLN cells. Group 3 received $0.5*10^6$ CD103$^{-/-}$ Tregs and $2*10^7$ OXA dLN cells. Injection and "blinding" of the experimenter were done as described in 3.5.1. On the next day (d6), the mice were challenged twice, once at the 0h mark and again 8h later. This double challenge was established in preliminary experiments and was necessary in order to elicit a strong enough ear-swelling response in reconstituted Rag-1$^{-/-}$ mice.

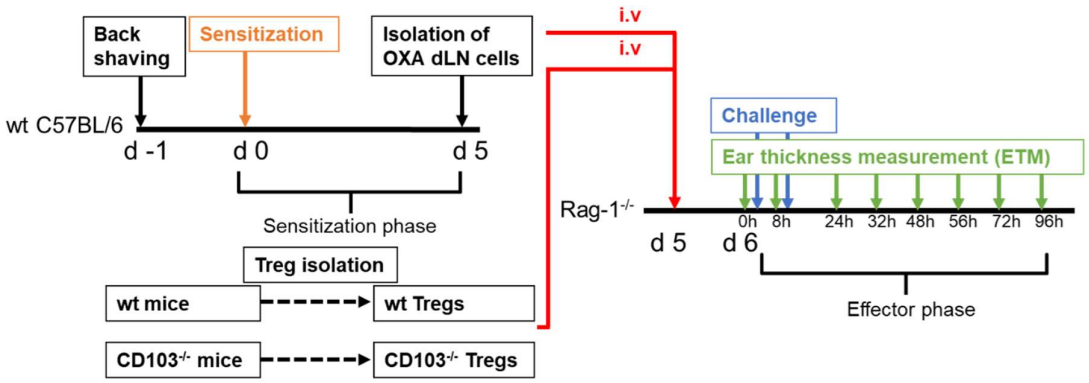

Figure 8: Treg transfer in reconstituted Rag-1$^{-/-}$ prior to the effector phase

3.6 Treatment protocol CD28 antibody, clone D665

The CD28-directed antibody (aCD28SA), clone D665, causes antigen-independent T-cell activation through crosslinking of CD28 molecules on the cell surface (Dennehy et al. 2006). It preferentially expands and activates murine Tregs (Gogishvili et al. 2009). We used this antibody to compare the activation capacity of Tregs in CD103$^{-/-}$ and wt C57BL/6 mice.

On d0, 200 µg of aCD28SA diluted with 300 µl PBS to a final volume of 500 µl was injected intraperitoneally in male CD103$^{-/-}$ and wt mice. Vehicle controls received 500 µl PBS. On d4, single cell suspensions of all skin-draining lymph nodes were prepared and analyzed by flow cytometry.

3.7 Flow cytometry

For fluorescence-activated cell scanning (FACS) the BD FACSCanto II Flow Cytometer and the BD FACSDiva Software Version 8.0.1were used. An unstained cell sample was used in every experiment to determine autofluorescence. All antibodies were tested against an appropriate isotype control to allow proper compensation (tables 5 and 6).

3.7.1 Intracellular FoxP3 staining protocol

The FoxP3 Fix/Perm Buffer Set from BioLegend was used for intracellular FoxP3 staining according to the manufacturer's protocol. All incubation steps were done under protection from ambient light to reduce the bleaching of fluorescent molecules. Cell viability was evaluated using the Zombie NIR™ Fixable Viability Kit. When lymph node samples were analyzed, 5*10^5 cells

per sample were stained. For isotype controls, $2.5*10^5$ were stained. All centrifugation was done at 1800 RPMI for 10 minutes at room temperature.

Initial transfer of the cells to FACS tubes was followed by centrifugation. After the removal of the supernatant, 100 µl per $1*10^6$ cells of 1 µg Zombie NIR™ in 100 µl PBS was added to the cells. The samples were then incubated at room temperature for 30 min. Afterwards, 2 ml of 0.1% FCS in PBS were added, followed by centrifugation. After partial aspiration of the supernatant (100 µl remained) and vortexing of the pellet, 1 µg per $1*10^6$ cells of a CD16/32-directed antibody were added and incubated for 5 minutes at 4°C. Thereafter, cells were incubated for 30 minutes at 4°C with antibodies against the following targets: murine TCRβ chain, CD4, CD8, CD25 and CD103 (Table 5). This was followed by two washing steps with 2 ml PBS each. During the last centrifugation, the fixation solution was prepared by diluting the fixation buffer at a ratio of 1:20 with cold PBS. After removal of the supernatant, under vortexing, 2 ml of the fixation solution per 10^6 cells were added, followed by incubation for 30 min at 4°C. Two more washing steps were performed. Next, the permeabilization solution was prepared by diluting the permeabilization buffer at a ratio of 1:5 with 37°C warm PBS. Again, while vortexing, 2 ml per 10^6 cells of permeabilization buffer were added. The samples were immediately centrifuged, and the permeabilization buffer was added one more time. Samples were then put into the drying oven at 37°C for 30 minutes. Afterwards tubes were washed two times. After vortexing, 1 µg per 10^6 cells of the CD16/32-blocking antibody were added to all samples and incubated for 5 min at 4°C. Now, the FoxP3 antibody was added and incubated for 30 min at 4°C (table 5). Two more washing steps concluded the staining.

3.8 Intradermal retention

In order to investigate whether CD103 is required for lymphocyte retention in the skin, we injected ears of $Rag1^{-/-}$ mice intradermally with a mix of wt and $CD103^{-/-}$ dLN cells. Prior to injection, the donor cells were stained with different cell-tracing dyes, either carboxyfluorescein succinimidyl ester (CFSE) or CellTrace™ Far Red. These dyes have non-overlapping emission spectra allowing the simultaneous tracing of two cell populations. Stainings were performed under protection from ambient light to minimize bleaching of fluorescent dyes. To guarantee a homogeneous staining, no more than $40*10^6$ cells were stained at a time.

CFSE staining was performed as follows: The wt dLN cell suspension was centrifuged and resuspended in PBS at a concentration of $20*10^6$ cells per 500 µl of PBS. Simultaneously, CFSE, which was stored at -20°C at a concentration of 10 mM, was freshly thawed and diluted with

PBS down to a concentration of 5 μM. Equal volumes of the wt dLN cell suspension and the CFSE solution were mixed, further lowering the CFSE concentration to the final concentration of 2.5 μM. The CFSE/cell mix was then placed into a water bath (30°C) for 8 minutes. The staining process was quenched through addition of twice the total staining volume of FCS. After two washing steps, live (trypan blue excluding) cells were counted in a Neubauer chamber.

CellTrace™ Far Red staining was carried out in parallel: The stock solution of 1 mM was freshly thawed. Per $20*10^6$ cells, 1 μl of stock solution was added to 1 ml of warm PBS. The dLN cells were centrifuged and the pellet was resuspended in the dye solution (1 ml per $20*10^6$ cells). The cell/dye mix was gently agitated for 2 min and then incubated for 20 min at room temperature. Quenching was achieved through addition of five times the staining volume of FCS. After two washing steps, the vital cells were counted in a Neubauer chamber. Next, equal numbers of both CFSE and CellTrace™ Far Red stained cells were mixed (1:1 ratio) and centrifuged. The pellet was resuspended at a concentration of $20*10^6$ per 100 μl PBS. The staining success and the exact ratio were determined by flow cytometry (CFSE was measured in the AmCyan channel and CellTrace™ Far Red in the allophycocyanin (APC) channel).

Using this cell mix, the right ears of Rag-$1^{-/-}$ mice were injected intradermally several times. A 1 ml syringe equipped with a 30-gauge cannula was used. The left ears were injected similarly with vehicle (PBS). The mice were killed the next day, and both ears were processed into single cell suspensions. The cell suspensions were analyzed by flow cytometry. A gate was set on potential lymphocytes based on the forward and sideward scatter. CFSE and CellTrace™ Far Red positive cells were then gated and the ratio between events of both populations calculated.

3.9 Data analysis and statistics

Microsoft Excel was used for basic data collection and statistical analysis. Student's T-test was used to test for statistical significance. A p value of less than 0.05 was considered to be significant. Graphs were created with Prism 6 for Windows V. 6.07. Microsoft PowerPoint was used to create figures. FACS analysis was performed using BD FACSDiva Software Version 8.0.1. Overlays of FACS Plots were created by using Adobe Photoshop.

4 Results

4.1 The role of CD103 for Treg regulation during sensitization

The research leading up to this thesis suggested that $CD4^+$ $CD25^+$ Tregs are impaired in their regulatory function in $CD103^{-/-}$ mice, thus causing increased CHS susceptibility (Braun et al. 2015). Generally, the importance of Tregs for the regulation of both sensitization and effector phase has been well established (see 1.3). We hypothesized that this regulatory function depends at least in part on CD103. We tested this hypothesis by comparing the suppressive effect of adoptively transferred wildtype and CD103-deficient $CD4^+$ $CD25^+$ Tregs either during sensitization or the effector phase (See 4.2).

4.1.1 Treg transfer prior to sensitization in wt mice

Transfer of wt Tregs prior to sensitization has been shown to suppress sensitization in a dose-dependent manner (Ring et al. 2010b). In order to examine if Tregs of $CD103^{-/-}$ mice are equally capable of suppressing sensitization, we injected groups of naive wt mice with either $0.5*10^5$ $CD103^{-/-}$ Tregs or $0.5*10^5$ wt Tregs prior to sensitization. The ear-swelling in the subsequent effector phase was used as an indicator for the sensitization success.

It was found that the ear-swelling responses of neither wt Treg or $CD103^{-/-}$ Treg treated groups differed significantly from the vehicle control (Figure 9). All groups displayed a similar degree of ear inflammation, indicating that neither wt nor $CD103^{-/-}$ Tregs suppressed sensitization. This result was surprising, since the findings of Ring et al. could not be reproduced. Transfer of $0.5*10^5$ wt Tregs should have at least partially suppressed sensitization according to their study.

In order to increase the suppressive impact of transferred Tregs without increasing the numbers of transferred Treg cells, DEREG mice were used as recipients of Treg transfers for all further studies on the sensitization phase. This was done in analogy to the approach of Ring et al., which aimed to deplete the endogenous Treg pool to better detect the effect of the transferred Tregs. For detailed discussion of the pros and cons of these approaches see 5.1.

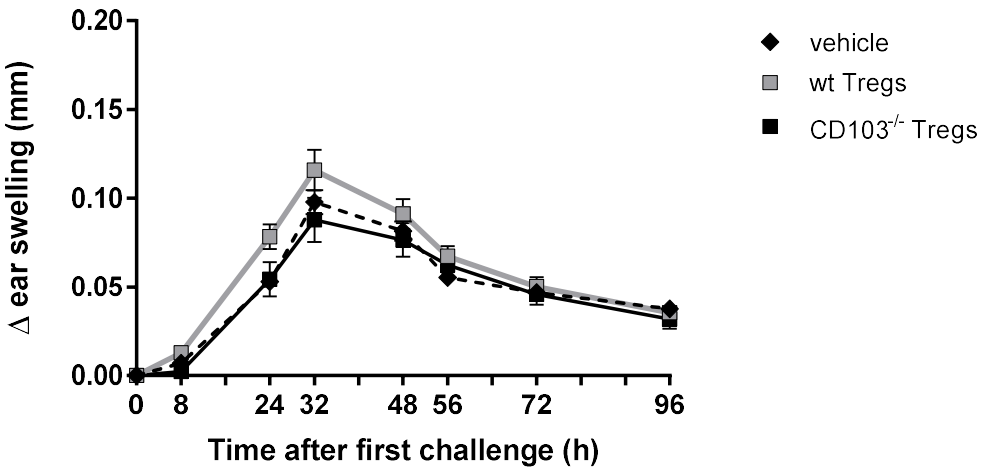

Figure 9: Transfer of wt Tregs failed to suppress sensitization.
wt mice were injected with either $0.5*10^6$ wt Tregs, $0.5*10^6$, $CD103^{-/-}$ Tregs, or PBS (vehicle) on day -1. The next day, the standard CHS protocol with 3%/1% OXA for sensitization/challenge and a 5-day lag time was initiated. Data points represent normalized differences in ear thickness between OXA- and vehicle-treated ears from 3 independent experiments (n = 5-11 mice per data point; mean ± standard error of the mean (SEM); see supplemental data (Figure A1) for the results of the individual experiments).

4.1.2 Treg-depleted DEREG mice as recipients of Treg transfers

DEREG (DEpletion of REGulatory T-cells) mice are a bacterial artificial chromosome (BAC) transgenic mouse line on a C57BL/6 background expressing a diphtheria toxin receptor (DTR) – enhanced green fluorescent protein (eGFP) fusion protein under the control of a FoxP3 promoter (Lahl et al. 2007). Therefore, all FoxP3-expressing cells inevitably coexpress the diphtheria toxin receptor, rendering these cells selectively vulnerable to diphtheria toxin. Administration of DT to these mice depletes all FoxP3-expressing cells. By using these Treg-depleted DEREG mice as recipients of Treg transfers we attempted to augment the impact of the transferred Tregs without having to increase the Treg cell numbers. The limitations of this approach are discussed in 5.1.1.

4.1.2.1 Treg depletion efficacy and Treg-recovery kinetics

First, the depletion kinetics of $CD25^+$ $FoxP3^+$ Tregs following a one-time DT application was analyzed. For that purpose, DEREG mice were injected intraperitoneally with 1 μg of DT, and the skin-draining lymph nodes were analyzed for $CD4^+$ $CD25^+$ $FoxP3^+$ regulatory T-cells after varying time intervals (3 hours up to 15 days).

Treg depletion started rapidly within hours after DT injection and peaked after about 24 hours (supplemental figure A2). The depletion efficacy at that point reached about 95%, with a reduction of $CD25^+$ $FoxP3^+$ cells amongst all $CD4^+$ cells from about 11% to about 0.5% (Figure 10).

When the duration of this depletory effect was investigated, Treg depletion in DEREG mice was found to be temporary. By day 5 after DT injection Treg counts recovered to about 60% of the status quo and normalized fully by day 12 (Figure 10).

This data helped us to set both the timing of sensitization after DT injection and the interval between sensitization and challenge (lag-time). Sensitization at the point of peak depletion (24 hours post DT injection) allowed for the strongest possible sensitization, because of the almost complete lack of Treg regulation. At the same time, the fact that Treg counts normalized by day 12 meant that initiation of the effector phase with a 12-day lag time would allow the effector phase to be unaffected by the preceding Treg depletion. This allowed selective investigation of the impact of Treg depletion on the sensitization phase independent from the effector phase.

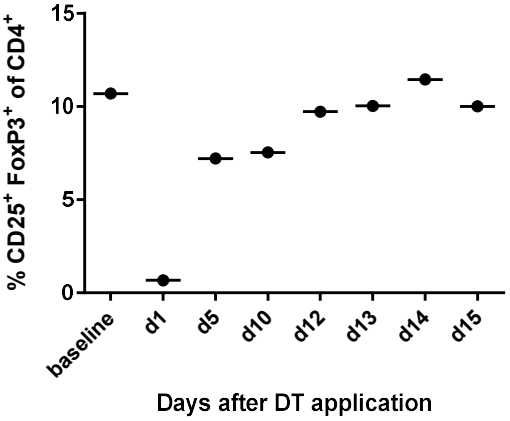

Figure 10: Treg long-term recovery kinetics after a single-shot DT application.
DEREG mice were injected with 1 µg of DT i.p. (d0). After different time intervals the mice were sacrificed and the frequency of $CD25^+$ $FoxP3^+$ on living $CD4^+$ cells in the draining lymph nodes was analyzed by flow cytometry. A vehicle-treated DEREG mouse was used to establish the baseline value. The frequency of $CD25^+$ $FoxP3^+$ cells on living $CD4^+$ cells is depicted (n = 1 per timepoint).

4.1.2.2 Adaptation of the CHS model in DEREG mice

After establishing the timing of sensitization after DT injection (d-1) and the length of the lag-time (12 d), the CHS model was tested with these parameters. Consistent with other studies, (Honda et al. 2011; Lehtimäki et al. 2012), the ear inflammation in Treg-depleted DEREG mice was strongly increased (Figure 11A). The ear inflammation was so severe that no resolution towards the later stages of the effector phase became apparent. In fact, the ear thickness kept

increasing over the entire course of the effector phase. This was mostly the result of excessive ear scaling, which appeared even at very early time points after challenge (Figure 11B). Furthermore, mice showed visible signs of distress throughout the effector phase. In light of the early and excessive ear scaling and the lack of resolution, the CHS response was deemed to be too severe. In order to decrease the severity, lower OXA concentrations were tested for sensitization and challenge.

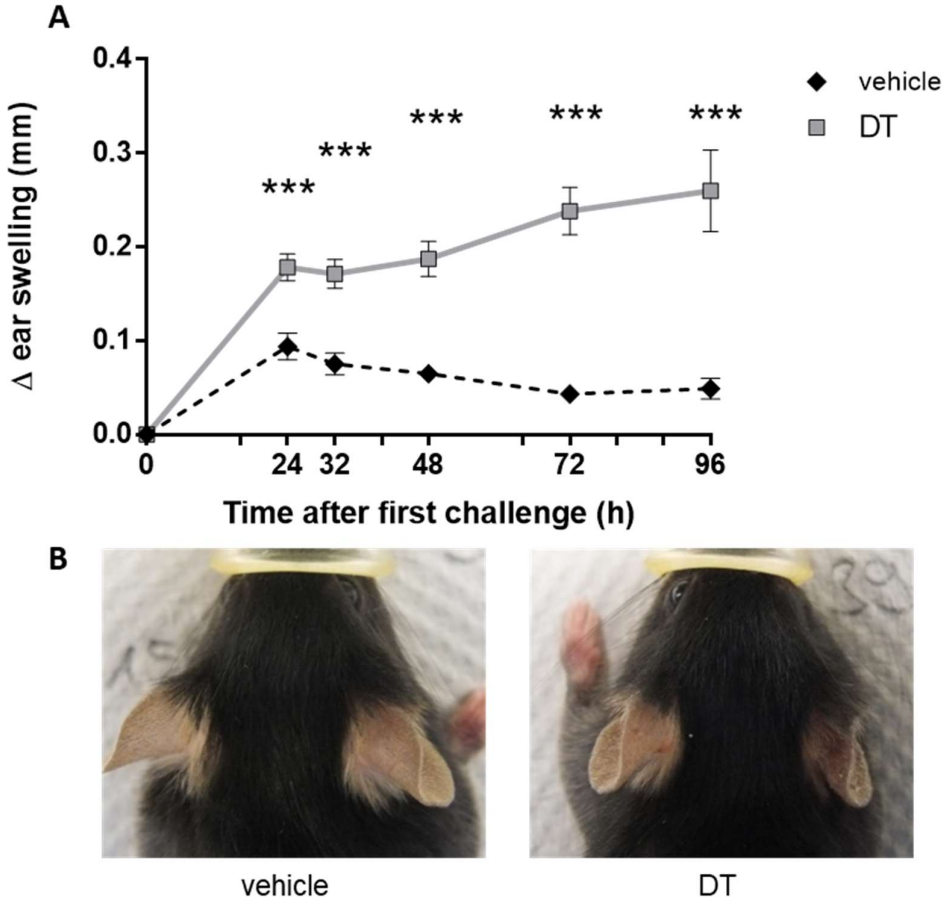

Figure 11: Sensitization/challenge with 3%/1% OXA causes severe inflammation in DEREG mice.
CHS was elicited in Treg-depleted DEREG mice using 3% OXA for sensitization and 1% OXA for challenge. A lag time of 12 days was chosen. Treg depletion was achieved through intraperitoneal injection of 1 µg DT in PBS 1 day prior to sensitization. The vehicle controls received only PBS. **A)** Data points represent normalized differences in ear thickness between the OXA-treated and the vehicle-treated ears (n = 10-12; mean ± SEM). *** $p < 0.001$ (unpaired Student's t test). **B)** Representative images of ear inflammation and scab formation 32 h post challenge.

In the following experiment the CHS responses towards the standard OXA concentrations of 3%/1% OXA for sensitization/challenge were compared with the reduced concentrations of

0.1%/1% (Figure 12). The 0.1%/1% group displayed the same numerical ear-swelling as the 3%/1% group, without the ear scaling (Figure 12). Furthermore, a significant resolution of the ear inflammation became apparent in later stages of the effector phase. Therefore, 1%/0.1% OXA were used for all further experiments with DEREG mice.

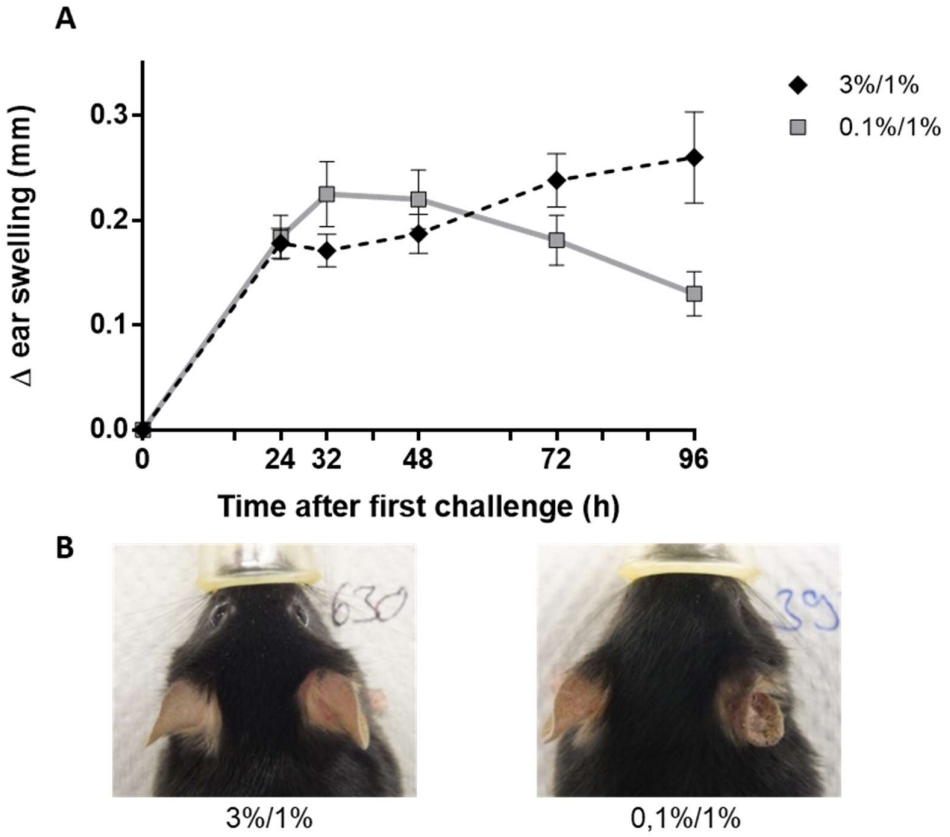

Figure 12: 0.1%/1% OXA allows for a strong ear-swelling response without scaling.
0.1%/1% OXA for sensitization/challenge was compared with the standard 3%/1% in Treg-depleted DEREG mice. Depletion was achieved through injection of 1 µg DT 1 day prior to sensitization. A 12-day lag time between sensitization and challenge was chosen. **A**) Data points represent normalized differences in ear thickness between the OXA-treated and the vehicle-treated ears (n = 3; mean ± standard deviation (SD)). **B**) Representative images of ear inflammation and scab formation 72 h post challenge.

4.1.3 Treg transfer prior to sensitization in Treg-depleted DEREG mice

Next, we determined whether $0.5*10^5$ wt Tregs were able to suppress sensitization in DEREG mice. For that purpose, groups of Treg-depleted DEREG mice were injected with either $0.5*10^6$, $1*10^6$ Tregs or vehicle (PBS), followed by the adapted CHS model (see 3.5.2 for the detailed experimental setup).

Indeed, from 24 h to 56 h post challenge both Treg treatment regimens significantly attenuated the ear-swelling response compared to the control group (Figure 13). These findings were further confirmed macroscopically (Figure 13B). The ears of Treg recipients were much less inflamed, as indicated by less erythema and less prominent vascularization. Most importantly, $0.5*10^6$ Tregs proved to be non-inferior to $1*10^6$ Tregs. Thus, using Treg-depleted DEREG mice as recipients of Treg transfers in conjunction with an adapted CHS model were able to reproduce and confirm the findings of Ring et al.

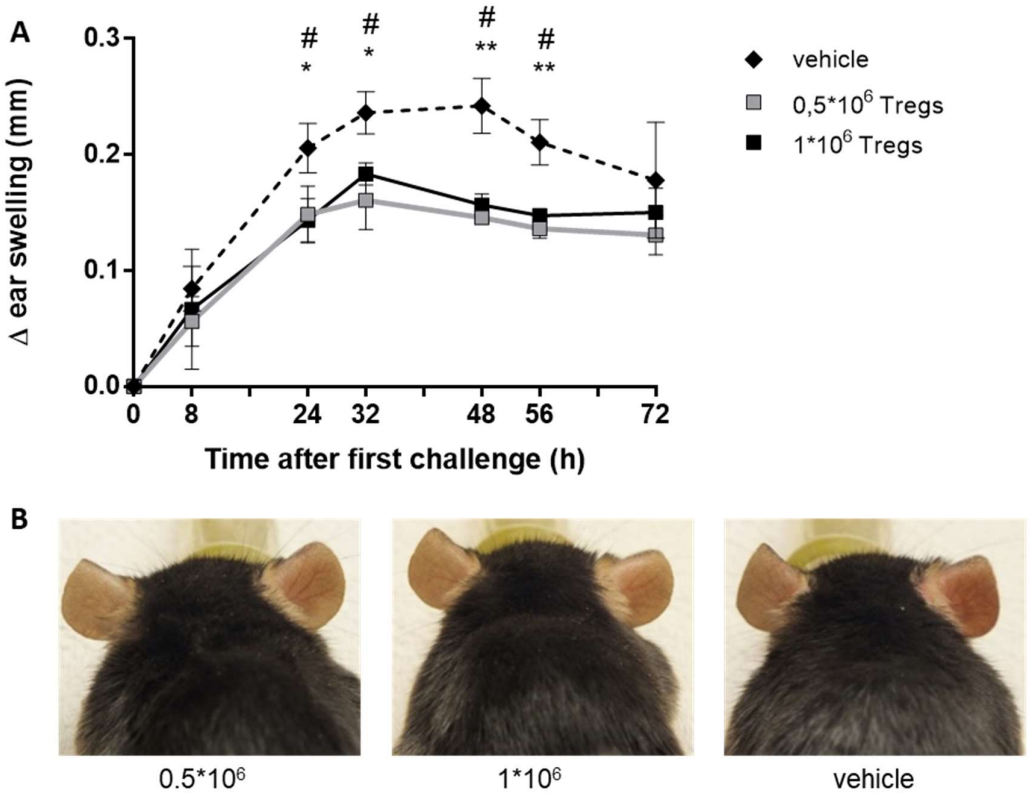

Figure 13: Transferred wt Tregs suppress sensitization in Treg-depleted DEREG mice. DEREG mice were injected with either $0.5*10^6$ Treg, $1*10^6$ Tregs or vehicle (PBS). 2 hours earlier Treg depletion was achieved through intraperitoneal injection of 1 µg DT. The next day, the adapted CHS model with 0.1%/1% OXA for sensitization/challenge and a 12-day lag time was initiated**. A)** Data points represent normalized differences in ear thickness between the OXA and the vehicle-treated ear (n = 3: mean ± SEM). *, # $p < 0.05$; **, ## $P < 0.01$; (unpaired Student's t test, *comparing the recipients of $0.5*10^6$ Tregs with recipients of vehicle, # comparing the recipients of $1*10^6$ Tregs with recipients of vehicle). **B)** Representative images of ear inflammation at 32 h post challenge.

After establishing a suitable experimental setup, it was investigated if $CD103^{-/-}$ Tregs were equally capable of suppressing sensitization as wt Tregs. For that purpose, wt Tregs and $CD103^{-/-}$ Tregs were transferred into Treg-depleted DEREG mice prior to sensitization (see 3.5.2 for

the detailed experimental setup). As expected (Figure 13), $0.5*10^6$ wt Tregs suppressed sensitization (Figure 14). The key finding was that DEREG mice injected with $CD103^{-/-}$ Tregs displayed an ear-swelling response indistinguishable from vehicle-treated mice, without any trend towards an attenuative effect of the $CD103^{-/-}$ Tregs. Thus, Tregs isolated from $CD103^{-/-}$ are not able to suppress sensitization. The ear-swelling-responses of wt Tregs and $CD103^{-/-}$ Tregs treated groups differed without reaching statistical significance (P of 0.13). Macroscopic images also suggested that $CD103^{-/-}$ Tregs failed to attenuate the ear inflammation, while wt Tregs clearly succeeded in doing so (Figure 14B). In conclusion, while Tregs from wt mice suppressed sensitization, Tregs from $CD103^{-/-}$ mice failed to do so. The regulatory function of Tregs during the sensitization phase seems to be impaired in $CD103^{-/-}$ mice.

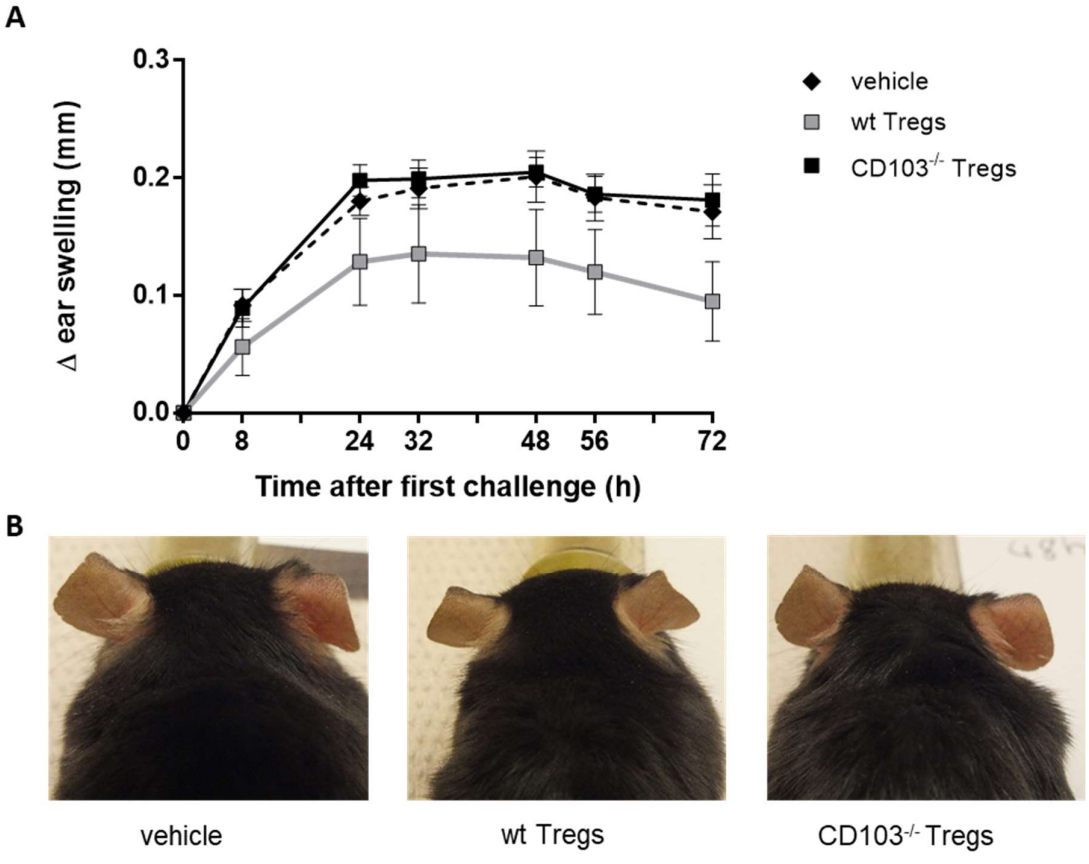

Figure 14: Transferred $CD103^{-/-}$ Tregs fail to suppress sensitization.
DEREG mice were injected with either $0.5*10^6$ wt Tregs, $CD103^{-/-}$ Tregs or vehicle (PBS). Two hours earlier, Endogenous Tregs were depleted through intraperitoneal injection of 1 µg DT. The next day, the modified CHS model with 0.1%/1% OXA for sensitization/challenge and a 12-day lag time was initiated. Photos taken documented the macroscopic ear inflammation. **A)** Data points represent normalized differences in ear thickness between the OXA challenged and the vehicle-treated ear (n = 3; mean ± SEM). **B)** Representative photos of ear inflammation 48 h post challenge.

4.2 The role of CD103 for Treg regulation during the effector phase

Tregs isolated from CD103$^{-/-}$ mice were not able to suppress sensitization. At least part of the aggravated CHS response observed in CD103$^{-/-}$ mice could be attributed to dysfunctional Treg regulation during the sensitization phase. This, however, does not rule out an additional impairment of Treg function during the effector phase. The general importance of Tregs during the effector phase has been established. Treg transfer before the effector phase has a suppressive effect on the ear-swelling response (Ring et al. 2006). In order to test whether this effect is abrogated in CD103$^{-/-}$ mice, the suppressive effect of wt Tregs was compared with CD103$^{-/-}$ Tregs transferred before challenge.

4.2.1 Treg transfer prior to the effector phase

Immunodeficient Rag1$^{-/-}$ mice were chosen as recipients of Treg transfers because they lack endogenous B and T-cells (Mombaerts et al. 1992). This trait creates a controlled environment inasmuch as T-cell-related findings can be attributed unambiguously to the transferred lymphocytes. However, this also meant that Rag-1$^{-/-}$ mice had to be reconstituted with dLN cells of previously OXA sensitized wt mice prior to the challenge (see 3.5.3 for the detailed experimental setup). The respective protocol had already been established in our lab.

In confirmation of previous studies (Ring et al. 2006), transfer of wt Tregs showed a suppressive effect on the ear-swelling response, particularly in the later stages of the effector phase (Figure 15), despite transferring only one tenth of the Treg numbers Ring et al transferred ($0.5*10^6$ vs $5*10^6$). By contrast, the CD103$^{-/-}$ Treg recipient group displayed an ear-swelling response indistinguishable from the control group. This indicated that CD103$^{-/-}$ Tregs failed to suppress the effector phase. In fact, the ear-swelling response of wt Treg recipients differed significantly from the CD103$^{-/-}$ treated group as early as 24 h after challenge. This indicated that Tregs in CD103$^{-/-}$ mice are also impaired in their regulatory role during the effector phase in addition to the sensitization phase.

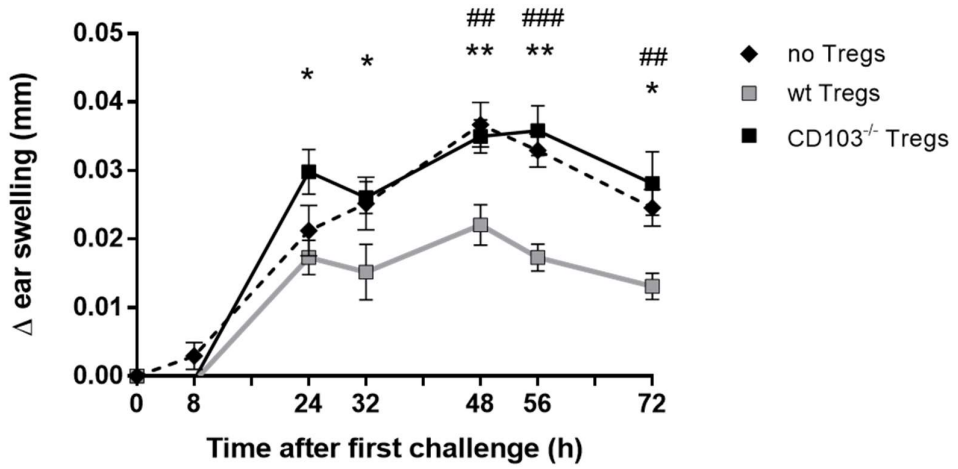

Figure 15: CD103$^{-/-}$ Tregs fail to suppress the ear-swelling response during the effector phase. Draining lymph node cells from previously sensitized wt mice (OXA dLN cells) were isolated on d5. 20*10^6 OXA dLN cells together with either 0.5*10^6 wt Tregs or CD103$^{-/-}$ Tregs were injected into Rag-1$^{-/-}$ mice. A control group received only 20*10^6 OXA dLN cells (no Tregs group). On the next day, Rag-1$^{-/-}$ mice were challenged twice (0 h and 8 h) with 1% OXA and the ear thickness was measured as usual. Data points represent normalized differences in ear thickness between the OXA and the vehicle-treated ear from two independent experiments (n = 8: mean ± SEM). **, ## $P < 0.01$; ***, ### $P < 0.001$ (unpaired Student's t test, *comparing the recipients of CD103$^{-/-}$ Treg cells with recipients of wt Treg cells, # comparing the recipients of wt Treg cells with no Tregs).

4.3 The role of CD103 for intradermal retention

A possible mechanism behind CD103 deficiency and the apparent dysfunction of CD103$^{-/-}$ Tregs is suggested by a murine model of Leishmaniasis, in which the dermal retention of CD4$^+$ CD25$^+$ near the site of infection was directly dependent on CD103 (Belkaid et al. 2002). Blockade of CD103 caused a marked decrease in the number of dermal Tregs.

It was conceivable that the regulatory role of Tregs during CHS could be similarly dependent on their dermal retention, which in turn could depend on CD103 expression. In order to test this hypothesis, the following experimental approach was devised: dLN cells from naïve wt and CD103$^{-/-}$ mice were stained with CFSE (wt dLN cells) or CellTrace™ FarRed (CD103$^{-/-}$ dLN cells) and the right ears of Rag-1$^{-/-}$ were injected intradermally with a 1:1 mix of these cells (see 3.8 for the detailed experimental setup). The exact baseline ratio of the injection solution was determined through flow cytometry (Figure 16A). The left ears served as a control and were injected with vehicle (PBS). The next day, the ears were analyzed for the remaining CFSE$^+$ and CellTrace™ FarRed$^+$ cells. The change in ratio between two cell populations served as readout parameter. Superior retention of CD103 competent cells would cause a ratio shift in their favor. This approach has the advantage of being independent of the exact cell numbers injected.

Indeed, two clearly demarcated populations of CFSE$^+$ and CellTrace™ FarRed$^+$ cells were detectable in the right ears at 24 h after injection (Figure 16B). At the same time, no CFSE$^+$ or CellTrace™ FarRed$^+$ events were detectable in the vehicle-treated ears (Figure 16C). There was no difference in retention between both populations at this point, as indicated by the unchanged ratio (Figure 16D). However, this does not preclude possible differences at later timepoints. These results established an elegant way of comparing *in vivo* retention of two different cell populations.

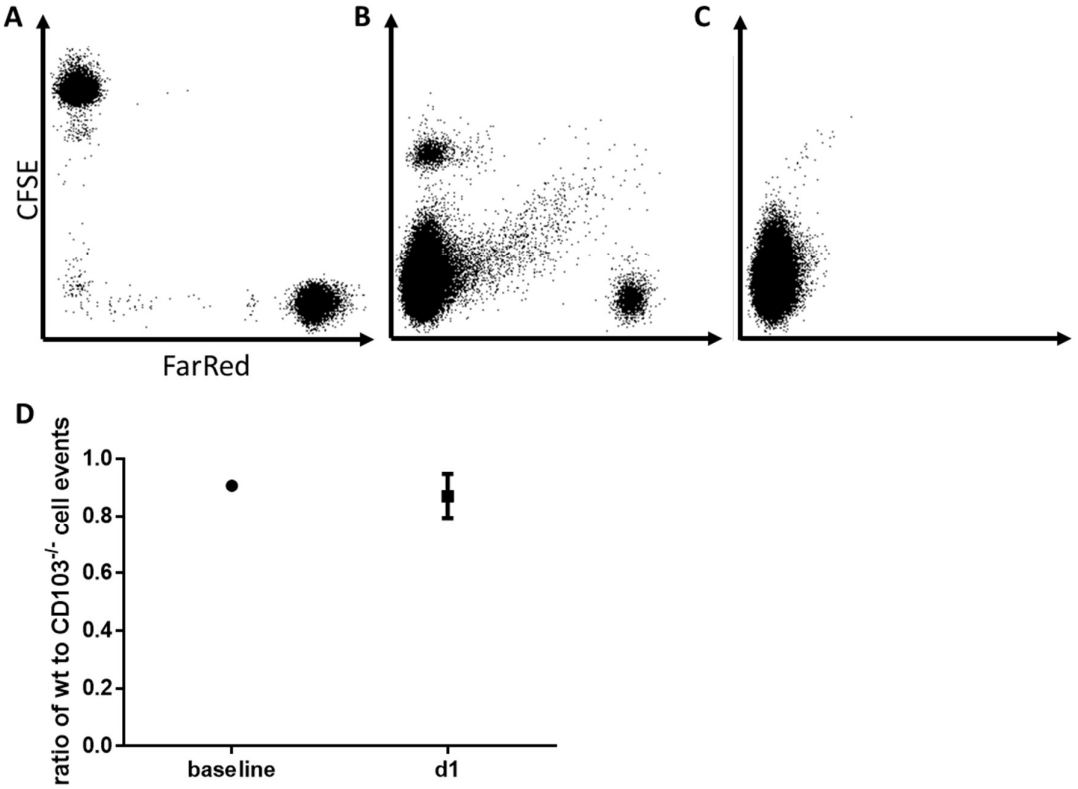

Figure 16: Intradermal retention
The right ears of Rag-1$^{-/-}$ mice were intradermally injected with a 1:1 mix of CFSE stained wt and CellTrace™ FarRed stained CD103$^{-/-}$ dLN cells. Left ears were injected with PBS (vehicle). 24 hours later, the ears were analyzed for residual cells through flow cytometry. The baseline ratio was determined prior to injection. CFSE$^+$ events were detected in the AmCyan channel, CellTrace™ FarRed$^+$ events in the APC channel. A gate was set on potential lymphocytes based on forward scatter (FSC) and sideward scatter (SSC). **A**) Pre-injection mix of CFSE$^+$ wt cells and CellTrace™ FarRed$^+$ CD103$^{-/-}$ cells **B/C**) FACS plot of an exemplary right ear (B) and a vehicle-injected left ear (C) 1 day after injection **D**) Calculated ratios between CFSE$^+$ and CellTrace™ FarRed$^+$ cells (mean ± SD; n=2).

4.4 Correlation of Treg activation and FoxP3 expression in CD103$^{-/-}$ mice

Preceding research of our group found that the FoxP3 expression of skin-residing CD4$^+$ CD25$^+$ cells during the effector phase was decreased in CD103$^{-/-}$ mice compared to wt mice (see 1.5)

(Braun et al. 2015). However, under steady-state conditions no abnormalities in Treg FoxP3 expression levels were observed in CD103$^{-/-}$ mice. Hence, it was hypothesized that the diminished FoxP3 levels indicated an impairment in the ability of CD103$^{-/-}$ Tregs to upregulate FoxP3 after activation.

To examine the ability of Tregs in CD103$^{-/-}$ mice to upregulate FoxP3, wt and CD103$^{-/-}$ mice were treated with the superagonistic CD28-directed antibody, D665. This antibody, through crosslinking surface CD28 molecules, preferentially expands and activates regulatory T-cells in a TCR-independent manner (Dennehy et al. 2006; Gogishvili et al. 2009).

4.4.1 Treg expansion in response to aCD28SA

Groups of wt mice and CD103$^{-/-}$ mice were injected intraperitoneally with vehicle (PBS) or 200 µg of aCD28SA (see 3.6) following a previously described regimen (Gogishvili et al. 2009). After 4 days, the mice were killed, and skin-draining lymph nodes were removed. Single cell suspensions from these lymph nodes were generated and flow-cytometrically analyzed (see 3.7 for the FACS staining protocol). First, we looked at the effect of aCD28SA on the draining lymph node cell numbers (Figure 17) and found the degree of cell expansion to be identical in both strains.

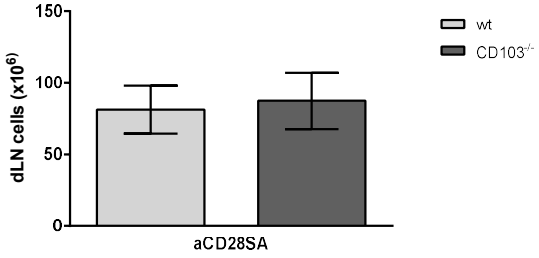

Figure 17: Similar lymphocyte counts in wt and CD103$^{-/-}$ mice after aCD28SA treatment.
Male wt and CD103$^{-/-}$ mice were treated with 200 µg aCD28SA. On d4, skin dLNs were sampled, processed into single cells suspensions and cells counted using trypan blue staining and a Neubauer chamber. (n = 3; mean ± SD).

Next, the impact of aCD28SA on the frequency of CD4$^+$ CD25$^+$ cells was assessed, since aCD28SA preferentially expands the CD4$^+$ CD25$^+$ cell subset (Gogishvili et al. 2009). Indeed, aCD28SA led to an expansion of the total percentage of CD4$^+$ CD25$^+$ cells in wt mice (Figure 18A). In these mice, CD4$^+$ CD25$^+$ cells made up more than 8% of all dLN cells, a 200% increase

compared to the vehicle-treated controls. This increase was caused by an increase in the proportion of $CD25^+$ cells on $CD4^+$ T-cells (Figure 18C). In aCD28SA-treated wt mice, 40% of $CD4^+$ cells expressed CD25, compared to 15% in the vehicle controls (Figure 18C). To make sure that the $CD25^+$ cells were not simply activated T-cells, FoxP3-expressing cells were assessed as well. And indeed, the total percentage of $CD4^+$ $CD25^+$ $FoxP3^+$ cells rose equally (Figure 18B). In fact, in wt mice, the proportion of $CD4^+$ $CD25^+$ cells expressing FoxP3 increased from 80% to 90% (Figure 18D). In contrast, in $CD103^{-/-}$ mice, no increase in the overall frequency of $CD4^+$ $CD25^+$ $FoxP3^+$ cells in response to aCD28SA was observed (Figure 18B). The relative percentage of $CD25^+$ cells on $CD4^+$ cells rose only to about 25% compared to the 15% of the vehicle controls (Figure 18C). At the same time, fewer $CD4^+$ $CD25^+$ cells expressed FoxP3 (Figure 18D). Still, this should have led to an increase in total percentage of $CD4^+$ $CD25^+$ cells. However, at the same time, the size of $CD4^+$ T-cell compartment diminished in comparison to wt mice (Figure 19). Of note, vehicle-treated wt and $CD103^{-/-}$ mice were identical in all parameters analyzed.

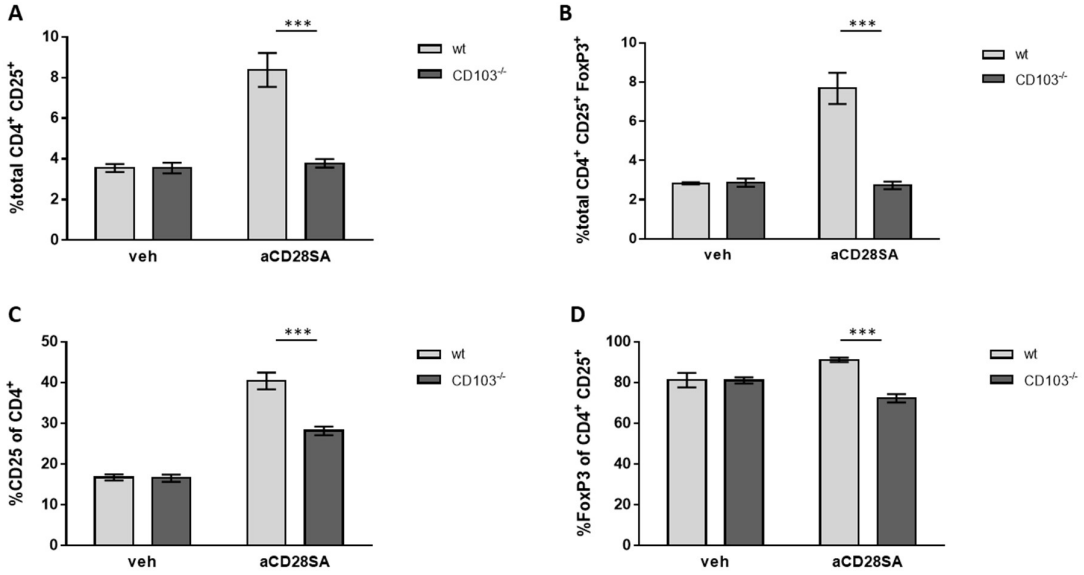

Figure 18: Treg expansion in $CD103^{-/-}$ in response to aCD28SA is abrogated.
Male wt and $CD103^{-/-}$ mice were injected with 200 µg aCD28SA. On d4 after treatment, dLN cells were prepared and stained for FACS analysis. Single cells were gated *via* FSC-A and FSC-H. Dead cells were excluded via Zombie NIR™ Fixable Viability Kit. Data was raised in two independent experiments.
A) Total percentage of $CD4^+$ $CD25^+$ cells. **B**) Total percentage of $CD4^+$ $CD25^+$ $FoxP3^+$ cells. **C**) Proportion of $CD25^+$ cells on all $CD4^+$ cells. **D**) Proportion of $FoxP3^+$ cells on $CD4^+$ $CD25^+$ cells. (n = 5-6; mean ± SEM; *** indicating significant difference, $P < 0.001$, unpaired Student's t test).

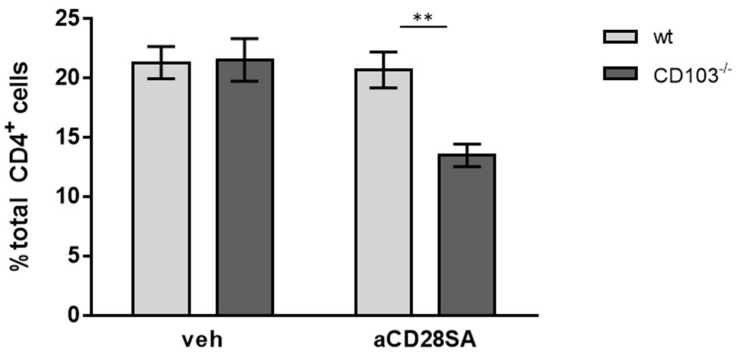

Figure 19: The CD4+ cell compartment decreases in CD103-/- mice in response to aCD28SA. Male wt and CD103-/- mice were injected with 200 µg aCD28SA. On d4 after treatment, dLN cells were prepared and stained for FACS analysis. Single cells were gated via FSC-A and FSC-H. Dead cells were excluded via Zombie NIR™ Fixable Viability Kit. Data was raised in two independent experiments. (n = 5-6; mean ± SEM; ** indicating significant difference, $P < 0.01$, unpaired Student's t test).

To summarize the above findings: flow cytometric analysis of the lymph nodes showed that aCD28SA treatment in wt mice led to a doubling of the Treg frequency. This translates to a doubling of the absolute Treg cell numbers, since total lymphocyte numbers were identical between treated CD103$^{-/-}$ mice and wt mice (Figure 17). In stark contrast, there was no increase in the frequency of CD4$^+$ CD25$^+$ FoxP3$^+$ cells in CD103$^{-/-}$ mice.

4.4.2 Expression level of CD25 and FoxP3 in response to aCD28SA

Next, the expression levels of CD25 and FoxP3 were investigated. There is evidence that CD103 expression is linked to higher FoxP3 expression levels (Lehmann et al. 2002; Hühn et al. 2004). Previous analysis of CD4$^+$ CD25$^+$ cells in lymph nodes and skin of CD103$^{-/-}$ mice under steady-state condition revealed no difference in FoxP3 and CD25 expression compared to wt mice (see 1.5) (Braun et al. 2015). However, CD4$^+$ CD25$^+$ cells in the challenged skin of CD103$^{-/-}$ mice showed diminished FoxP3 expression.

In this setting, it was found that aCD28SA treatment led to an almost twofold increase in the CD25 mean fluorescence intensity (MFI) of CD4$^+$ CD25$^+$ cells in wt mice (Figure 20A). aCD28SA caused more CD4$^+$ cells to express CD25, and these cells expressed CD25 much more strongly (Figure 20B). A similar observation was made looking at the FoxP3 MFI of CD4$^+$ CD25$^+$ FoxP3$^+$ Tregs. The expression of FoxP3 doubled upon aCD28SA treatment, as indicated by a twofold increase in MFI (Figure 20C/D). In stark contrast, no such findings were made in aCD28SA-treated CD103$^{-/-}$ mice. The increase in CD25 MFI was negligable (Figure 20A). The FoxP3 upregulation was also much less pronounced. FoxP3 MFI increased only by

a factor of 1.3 (Figure 20C). Vehicle-treated mice from both strains were indistinguishable from each other in all regards. Differences became apparent only after Treg activation.

The diminished FoxP3 upregulation of CD103$^{-/-}$ Tregs in response to aCD28SA supported the hypothesis that FoxP3 upregulation after Treg activation is impaired in CD103$^{-/-}$ mice. This finding is in line with the previous finding that FoxP3 expression was diminished in the skin of challenged CD103$^{-/-}$ mice (Braun et al. 2015). However, the fact that the overall response to aCD28SA was almost completely abrogated, suggested that not only the FoxP3 upregulation was impaired, but Treg activation itself.

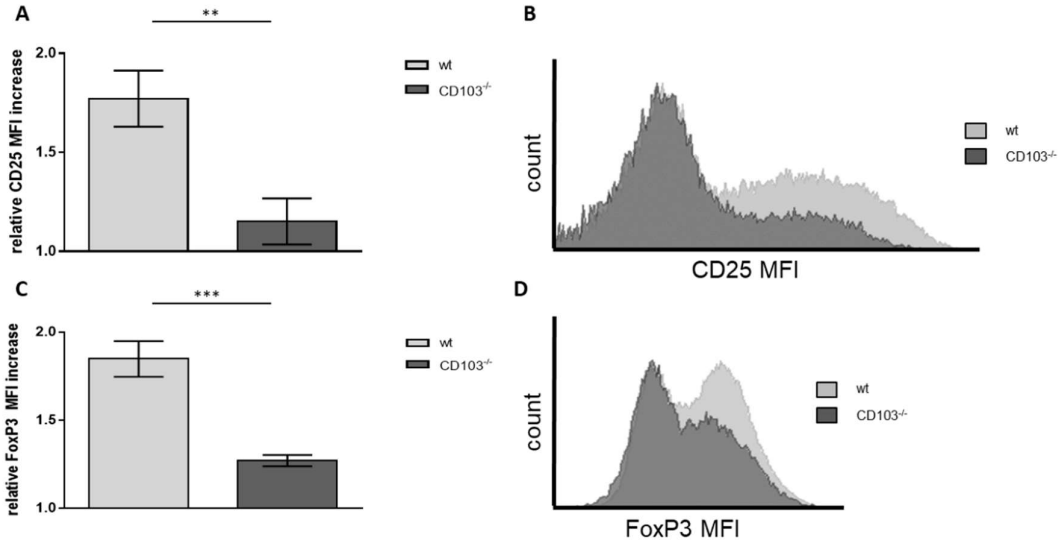

Figure 20: Tregs in CD103$^{-/-}$ mice fail to upregulate CD25 and FoxP3 in response to aCD28SA. Male wt and CD103$^{-/-}$ mice were injected with 200 µg aCD28SA. On d 4 after treatment, dLN cells were prepared and analyzed by FACS. Single cells were gated via FSC-A and FSC-H. Dead cells were excluded via Zombie NIR™ Fixable Viability Kit. Data was raised in two independent experiments.
A) Ratio of CD25 MFI of CD4$^+$ CD25$^+$ cells from treated mice and vehicle control **B**) Overlay showing CD25 histograms of treated CD103$^{-/-}$ and wt mice in direct comparison. **C**) Ratio of FoxP3 MFI of CD4$^+$ CD25$^+$ FoxP3$^+$ cells from treated mice and vehicle controls **D**) Overlay showing FoxP3 histograms of treated CD103$^{-/-}$ and WT mice in direct comparison. (n = 5-6; mean ± SEM; *** indicating significant difference, $P < 0.001$, unpaired Student's t test).

4.4.3 aCD28SA preferentially expands CD103$^+$ Tregs in wt mice

CD103 is commonly viewed as a marker for Treg of an effector/memory phenotype (Chang et al. 2012; Hühn et al. 2004; Lin et al. 2009). In accordance, treatment with aCD28SA led to an increase in the proportion of CD103 expressing CD4$^+$ CD25$^+$ FoxP3$^+$ cells in wt mice (Figure 21 A). Thus, CD103 induction corresponds to an activated phenotype, as was expected after aCD28SA treatment.

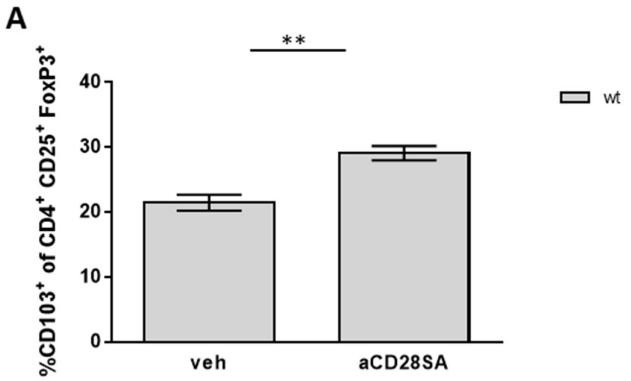

Figure 21: aCD28SA treatment expands CD103$^+$ Tregs in wt mice.
Male wt and CD103$^{-/-}$ mice were injected with 200 µg aCD28SA. On d4 after treatment, dLN cells were prepared and stained for FACS analysis. Single cells were gated *via* FSC-A and FSC-H. Dead cells were excluded *via* Zombie NIR™ Fixable Viability Kit. Data was obtained in two independent experiments. **A**) Proportion of CD103$^+$ cells on CD4$^+$ CD25$^+$ FoxP3$^+$ cells (n = 5-6; mean ± SEM; ** indicating significant difference, $P < 0.01$, unpaired Student's t test).

5 Discussion

5.1 Treg regulation of the sensitization phase

5.1.1 Treg transfer prior to the sensitization phase

In the first part of this thesis, the hypothesis was tested that part of the increased CHS susceptibility of $CD103^{-/-}$ mice is caused by an impairment in the regulatory function of Tregs in the sensitization phase. Indeed, Tregs from $CD103^{-/-}$ mice were unable to suppress sensitization (4.1.3).

The general importance of Tregs for the regulation of the sensitization phase has been well-established. Antibody-mediated depletion of $CD4^+$ T-cells prior to sensitization, which inevitably includes depletion of $CD25^+$ Tregs, aggravates the CHS response (Gocinski and Tigelaar 1990; Kish et al. 2005). More selective targeting, either by CD25-directed antibodies or through the even more selective usage of hCD52 reporter mice, delivered similar findings (Kish et al. 2005; Honda et al. 2011; Lehtimäki et al. 2012). In fact, Treg depletion enables the sensitization towards "weak" contact allergens, normally unable to elicit CHS, thus highlighting the importance of Tregs for immunotolerance during sensitization (Vocanson et al. 2006). The research so far suggests that this regulatory effect is mainly conveyed by Tregs located in the respective skin-draining lymph nodes, through cell contact-dependent mechanisms (Ring et al. 2010b). A large subset of Tregs in skin-draining lymph nodes (about 30%) actually expresses CD103 (Braun et al. 2015; Banz et al. 2003). Transfer of Tregs isolated from these lymph nodes has been shown to suppress sensitization in a dose-dependent manner (Ring et al. 2010b).

We tested whether this suppressive effect depends on CD103 expression comparing the suppressive effect of wt Tregs and $CD103^{-/-}$ Tregs transferred into wt mice previous to sensitization (4.1.1). Unexpectedly and in contradiction to a previous report (Ring et al. 2010b), the suppressive impact of transferred wt Tregs could not be reproduced. This apparent discrepancy might be explained by the fact that Ring et al. (2010b) treated recipients of Treg transfers 4 days previously with a depletory CD25 antibody. This antibody leads to the depletion of the endogenous $CD25^+$ Treg pool, which augmented the CHS response and at the same time amplified the impact of the $0.5*10^5$ transferred wt Tregs. It is reasonable to assume that in the setup of the present study with the endogenous Treg pool intact $0.5*10^5$ Tregs were too few cells to significantly affect sensitization. This meant that either more cells have to be injected or the effect of $0.5*10^5$ Tregs would have to be augmented, analogous to the depletory CD25 antibody approach.

5.1.2 DEREG mice as recipients of Treg transfers

The depletory CD25 antibody approach utilized by Ring et al. has some limitations in terms of specificity and efficacy. While CD25 is an excellent surface marker for regulatory T-cells, it is neither 100% sensitive nor completely specific (Chen and Oppenheim 2011). Regulatory T-cells are much better characterized by the transcription factor FoxP3 (Fontenot et al. 2003). Moreover, CD25 is not selectively expressed by regulatory T-cells, but also by activated cytotoxic $CD8^+$ T-cells (Boyman and Sprent 2012), leading to co-depletion of these cells and, consecutively, a broader manipulation of the immune system. Furthermore, the depletion efficacy of the CD25 antibody approach is fairly low, with a drop in the frequency of splenic $CD4^+$ $CD25^+$ cells from about 15% to only about 5% (Couper et al. 2007). This translates to a depletion rate of only 66%. In light of these limitations, DEREG mice were chosen for the present study.

BAC transgenic DEREG mice possess an additional modified FoxP3 gene locus with the gene for a DTR–eGFP fusion protein inserted into exon 1 (Lahl et al. 2007). Consequently, cells expressing FoxP3 inevitably coexpress the DTR-eGFP construct, rendering them selectively vulnerable to the cytotoxic effects of DT. Thus, administration of DT to these mice allows targeted and efficient depletion of $FoxP3^+$ regulatory T-cells, which resulted in the use of these mice in many studies (Klages et al. 2010; Teng et al. 2010; Chenna Narendra et al. 2018).

However, there are clear limitations to this approach as well: A small percentage of $FoxP3^+$ cells (2-5%) is DT resistant, limiting the depletion efficiency (Lahl and Sparwasser 2011; Mayer et al. 2014). The present study confirmed these findings (4.1.2). While a high depletion efficacy of about 95% was reached, about 5% of FoxP3-expressing cells were DT resistant. It can be argued that the incomplete Treg depletion is actually an advantage, since complete depletion causes a devastating autoimmune disease (Kim et al. 2007), which would limit the practicability of such a mouse model.

In terms of timing, the depletion efficacy peaked at about 24 h after DT injection (4.2.2). Since the impact of transferred Tregs should in theory be greatest when the endogenous Treg numbers are at their lowest, sensitization should best be carried out 24 hours after DT administration. Furthermore, Treg migration to the draining lymph nodes peaks at 24 hours after injection into the bloodstream (Ring et al. 2006). Hence, carrying out DT injection and Treg transfer about 24 hours before sensitization should ensure maximal suppressive impact.

In confirmation of a study by Lehtimäki et al. (2012), Treg depletion prior to sensitization caused a massively increased CHS response (4.2.2). In contrast to Lehtimäki et al. (2012) however, the transiency of the depletory effect was exploited and the time interval between sensitization and

challenge was stretched to 12 days (4.2.2). This allowed endogenous Tregs to recover before elicitation of the effector phase. Lehtimäki et al. (2012) initiated the effector phase 6 days after DT application. At that point the $CD4^+$ $FoxP3^+$ were still down by more than 50% (Lehtimäki et al. 2012), meaning that Treg depletion potentially affected not only sensitization, but also the effector phase. Whether this had a measurable effect cannot be discerned from the data. The ear-swelling responses in the present and their study cannot be directly compared because of methodological differences. Lehtimäki et al. depicted absolute ear thicknesses in contrast to the difference in ear thickness between a vehicle-treated and a challenged ear.

Strikingly, using the standard CHS protocol the resulting ear inflammation was so severe that the decline of the ear-swelling response disappeared (See 4.2.2). No resolution of the inflammation towards the end of the effector phase was observed. Contrary to this, in the study by Lehtimäki et al. the ear-swelling response decreased visibly at the 96 h mark. This discrepancy can be explained by lower OXA concentration of 1% for sensitization and 0.3% for challenge utilized by Lehtimäki et al. (Lehtimäki et al. 2012). Because of this lack of resolution, and the excessive ear scaling which prevented reliable ear thickness measurement, the OXA concentrations for both sensitization and challenge were lowered (4.2.2). Indeed, the CHS response towards 0.1%.1% OXA, while still being strongly aggravated, showed the normal bell-like shape, indicative of resolving inflammation. Furthermore, the excessive ear scaling disappeared.

5.1.3 Tregs in $CD103^{-/-}$ mice fail to suppress sensitization

By using Treg-depleted DEREG mice to augment the impact of $0.5*10^6$ transferred Tregs, in conjunction with the adapted CHS protocol (see 3.5.2), the suppressive effect of wt Tregs on sensitization was confirmed (Ring et al. 2006; Ring et al. 2009). At the same time, with wt Tregs as positive control, Tregs from $CD103^{-/-}$ mice were unable to suppress sensitization (4.2.3).

Going back to the initial observation that prompted this thesis: This result shows that part of the increased CHS susceptibility of $CD103^{-/-}$ mice can be attributed to an impairment in the regulation of the sensitization phase by Tregs. These findings are not totally surprising and without precedent. In a murine model of inflammatory bowel disease only $CD103^+$ $CD25^+$ Tregs were able to control the disease, whereas $CD103^-$ $CD25^+$ Tregs did not show any protective effects whatsoever (Banz et al. 2003). Other studies similarly support a model in which the CD103 expressing $CD25^+$ Tregs convey the bulk of the regulatory function *in vivo* and *in vitro* (Lehmann et al. 2002; Hühn et al. 2004). These studies, however, all presented circumstantial evidence only. Lehmann et al. and Banz et al. compared the suppressive capacities of sorted $CD103^+$ Tregs and $CD103^-$ Tregs, therefore not showing a direct functional relevance of CD103

(Banz et al. 2003; Lehmann et al. 2002). As a matter of fact, in a murine colitis model $CD103^{-/-}$ Tregs ameliorated the colitis of recipient mice as proficiently as wt Tregs, implying that CD103 expression is actually dispensable for Treg function, at least in this context (Annacker et al. 2005). This gave rise to the concept that CD103 is merely a marker for an activated Treg phenotype. $CD103^{+}$ Tregs in skin-draining lymph nodes have emigrated from the skin (Tomura et al. 2010). These migratory $CD103^{+}$ Tregs displayed particularly strong suppressive activity both *in vitro* and *in vitro*, further suggesting that CD103 is acquired upon activation in the periphery.

This study provides evidence that CD103 is not simply a marker for activated Tregs, but also relevant for their regulatory function during sensitization. Interestingly, a recent study found that $CD103^{-/-}$ mice displayed aggravated airway inflammation in an asthma model (Fear et al. 2016). Unfortunately, this study did not investigate Treg functions in this context.

A causal link between CD103 deficiency and impaired function of Tregs has not been proven. Treg dysfunction could, in principle, be caused indirectly by other ramifications of CD103 deficiency, such as altered Treg development. Again, $CD103^{-/-}$ Tregs have been shown in other contexts to be fully functional (Annacker et al. 2005). Establishing a causal relation would require functional inhibition of CD103. For example, an inhibitory antibody could be administered to isolated wt Tregs prior to transfer. If CD103 inhibition is able to abrogate the suppressive effect of wt Tregs, this would underscore a causal link between CD103 expression and impaired suppression. CD103 knockdown in isolated wt Tregs would be another option.

Assuming that CD103 is directly involved in Treg regulation during sensitization, what are possible mechanisms? A role for CD103 in the retention of T-cells in general has been shown in several studies (Hardenberg et al. 2018). For Tregs, however, it has only been shown in leishmania skin infection (Suffia et al. 2005). Still, altered retention is an obvious candidate. As CD103 is almost uniformly expressed on dermal Tregs, a role for dermal retention appears likely. However, no differences in the frequencies of dermal $CD4^{+}$ $CD25^{+}$ Tregs between wt and $CD103^{-/-}$ mice under both steady-state and inflammatory conditions were found (Braun et al. 2015). Importantly, involvement of dermal Tregs in the regulation of the sensitization phase has not been described. The research so far shows that Treg regulate sensitization primarily through cell contact-dependent mechanisms in the dLN (See 1.3). Accordingly, impaired or delayed accumulation of $CD103^{-/-}$ Tregs in the dLN could mediate the impaired function. As the suppression of sensitization directly depended on the numbers of Tregs within the lymph nodes (Ring et al. 2010b), decreased accumulation would result in decreased suppressive capacity. However, no alterations in Treg counts in the skin dLN of $CD103^{-/-}$ mice were detected in both steady-state and inflammatory conditions (Braun et al. 2015). Furthermore, lymph node

engraftment of wt Tregs and CD103$^{-/-}$ Tregs after injection into SCID mice was found to be identical, albeit in a model of chronic leishmania skin infection (Suffia et al. 2005). This left only the possibility that, while CD103$^{-/-}$ Tregs eventually settle equally well in the draining lymph nodes, they might do so at a slower pace. This could be investigated in future studies by comparing the draining lymph node migration kinetics of wt and CD103$^{-/-}$ Tregs.

5.2 Treg regulation during the effector phase

Similar to the sensitization phase, Tregs are generally relevant for the regulation of the effector phase. Their depletion in the effector phase aggravated ear inflammation (Tomura et al. 2010; Lehtimäki et al. 2012). *Vice versa*, transfer of exogenous Tregs prior to challenge suppressed the ear-swelling response (Ring et al. 2006). The role of CD103 in this respect was studied by comparing the capacity of transferred wt and CD103$^{-/-}$ Tregs to suppress the challenge reaction. Indeed, as seen in the sensitization phase, transferred wt Tregs exerted this function while CD103$^{-/-}$ Tregs did not (4.3). This suggested that Treg dysfunction in both phases contributes to the increased CHS susceptibility of CD103$^{-/-}$ mice.

The research so far found that Tregs regulate sensitization and effector phase through fundamentally different modes of action. The regulation of the sensitization phase was shown to be mediated mainly through cell contact-dependent mechanisms (Ring et al. 2010b), whereas the regulation of the effector phase was mediated by soluble factors (Ring et al. 2010a). The present study suggests that CD103-dependent suppression is relevent in both phases. Once again, this must be interpreted with caution, since no direct causal link between CD103 deficiency and Tregs function was established. Moreover, the fact that Tregs from CD103$^{-/-}$ mice were dysfunctional in both phases could be seen as evidence for a broader CHS-independent dysfunction of Tregs in CD103$^{-/-}$ mice. This will be discussed in 5.4.

How could CD103 mediate the suppressive effect of Tregs in the effector phase? In this and other studies (Tomura et al. 2010; Lehtimäki et al. 2012), wt Tregs were primarily involved in the regulation of the later stages of the effector phase. This coincides with a higher frequency of FoxP3^{+} cells in the skin (Lehtimäki et al. 2012). Lehtimäki et al. found that 24 h after challenge about 15% of T-cells in the skin stained positive for FoxP3, whereas this number increased to more than 40% at 96 h after challenge. This suggests that Tregs facilitate the resolution of inflammation by accumulating in the challenged skin during the effector phase.

Of note, so far the investigations on the mechanisms of Treg regulation in the effector phase have shown no necessity for direct Treg presence in the skin. Instead, they showed that the

suppressive effect is independent of Treg localization and is rather mediated by soluble factors, most importantly IL-10 (Ring et al. 2006). Ring et al. examined whether transferred Tregs infiltrate the inflamed skin in order to exhibit their regulatory function in situ (Ring et al. 2006). They tried tracing injected Tregs with the PKH26 dye but failed to detect any $PKH26^+$ cells in the ears at up to 48 h post challenge. However, the observation that transferred Tregs home to the skin questions the sensitivity of their approach (Dudda et al. 2008; Suffia et al. 2005).

5.3 The role of CD103 for dermal Treg accumulation

Impaired accumulation would plausibly explain the inability of Tregs in $CD103^{-/-}$ mice to suppress the effector phase. In general, CD103 could control Treg accumulation through regulating either recruitment to or retention within the skin. Skin resident Tregs almost uniformly express CD103, suggesting that it does play some role (Braun et al. 2015; Banz et al. 2003). For $CD8^+$ T-cells, experimental evidence argues against a role of CD103 for cell recruitment (Hardenberg et al. 2018). Rather, CD103 was crucial for long-term retention of cells in tissues. Mackay et al. conclusively showed this in herpes simplex skin infection (Mackay et al. 2013). CD103 competent and CD103 deficient T-cells infiltrated the epidermis equally well, but over time the ratio of cells started to skew heavily towards the CD103 competent population.

The present study investigated whether cutaneous Tregs numbers were diminished in $CD103^{-/-}$ mice under steady-state and inflammatory conditions in the effector phase, but found no abnormalities up to 24 hours after challenge (Braun et al. 2015). However, based on the findings of Lethämkäi et al., later timepoints might have yielded different results.

In the same study, our group proposed a role of CD103 for Treg accumulation in challenged skin (Braun et al. 2015). When CHS was elicited in radiated Balb/c mice reconstituted with a 1:1 mixture of bone marrow from wt ($Thy1.1^+$) and $CD103^{-/-}$ ($Thy1.2^+$) donors, the ratio of $Thy1.1^+$ and $Thy1.2^+$ was skewed significantly towards wt Tregs at 96 h post challenge (Braun et al. 2015). Thus, Tregs in $CD103^{-/-}$ mice are impaired in their accumulation in challenged skin. However, this being a correlation does not prove whether it is a direct consequence of CD103 deficiency. This aspect needs to be addressed in future studies.

A direct role of CD103 for the retention of Tregs in the dermis has been shown in chronic leishmania infection (Suffia et al. 2005). It was unclear whether these findings hold true in the context of CHS. The previous study examined the role of CD103 for dermal retention by injecting CFSE stained $CD4^+$ lymphocytes directly in the dermis (Suffia et al. 2005). After 24 h, $CD4^+$ lymphocytes from $CD103^{-/-}$ mice were not retained in the dermis, neither in the steady-

state nor during chronic leishmania skin infection. Furthermore, retention of $CD4^+$ lymphocytes from wt mice was abrogated in the presence of a CD103-blocking antibody, showing that CD103 is required for intradermal retention of $CD4^+$ cells. However, this approach was based on multiple intradermal injections of precise cell numbers. In our experience, reliably injecting precise cell numbers intradermally is very difficult and prone to errors. Thus, in the present study a 1:1 mix of $CD103^{-/-}$ and wt cells stained with different tracing dyes was injected. This allowed to analyze change of the ratio of the two cell types. No difference in dermal retention was detected after 24 h. Future investigations should address later time points. A role of CD103 for dermal retention always raises the question of the interaction partner, since E-cadherin as the only known CD103 ligand is not expressed in the dermis. Indeed, there is evidence for another yet unidentified CD103 ligand, not only on keratinocytes (Jenkinson et al. 2011; Brown et al. 1999), but also with the dermal compartment

5.4 Impaired Treg activation in $CD103^{-/-}$ mice

Research preceding this thesis found the FoxP3 expression levels of dermal Tregs in $CD103^{-/-}$ mice to be diminished during the effector phase compared to wt mice, while no such discrepancies were observed in the steady-state (Braun et al. 2015). CD103 expression and FoxP3 expression have long been known to be correlated. $CD103^+$ Tregs express higher FoxP3 levels than their $CD103^-$ counterparts (Hühn et al. 2004; Lehmann et al. 2002). The increased FoxP3 and CD103 expression levels are commonly regarded to be part of an activated Treg phenotype. It is possible that CD103 is involved in FoxP3 upregulation after Treg activation. Alternatively, decreased FoxP3 expression could be evidence of impaired Treg activation. Since the level of FoxP3 expression is linked to their suppressive function (Wan and Flavell 2007), this could provide another explanation for the increased CHS susceptibility of $CD103^{-/-}$ mice. This hypothesis was investigated by comparing the response of Tregs towards a superagonistic CD28 antibody both in wt and $CD103^{-/-}$ mice (4.4). This aCD28SA antibody induces TCR-independent T-cell activation through bivalent crosslinking of CD28 molecules, (Dennehy et al. 2006). This TCR-independent activation causes preferential activation and expansion of the $CD25^+$ Treg subset (Lin and Hunig 2003). It does not induce conversion of $CD25^-$ T-cells, but rather proliferation of preexisting $CD25^+$ cells (Gogishvili et al. 2009). This unique ability to preferentially manipulate the Treg compartment led to its application in several murine autoimmune disease models (Hunig and Dennehy 2005). Promising preclinical results led to a phase 1 trial, which unfortunately ended in a fatal cytokine storm in all six volunteers (Suntharalingam et al. 2006).

First, it was confirmed here that there were no differences in Treg frequency and Treg phenotype between naive wt and CD103$^{-/-}$ mice (4.4). Likewise, the proposed effect of aCD28SA in wt mice was confirmed. The Treg compartment in wt mice expanded massively and at the same time Tregs upregulated CD25 and FoxP3. Contrary to that, Tregs in CD103$^{-/-}$ mice did not only fail to upregulate FoxP3, as was the hypothesis, but also failed to upregulate CD25 and to proliferate (4.4). Strikingly, response to aCD28SA was almost completely abrogated in CD103$^{-/-}$ mice. Once again, it was not proven that CD103 deficiency is causally linked to the abrogated aCD28SA response. For example, CD103 deficiency could have led to compensatory changes in other molecules which mediate the abrogated response. To show a direct role of CD103, the response of wt mice to aCD28SA could be tested in the presence of a blocking CD103 antibody. The abrogated aCD28SA response in CD103$^{-/-}$ mice was viewed as a failure of the antibody to fully activate Tregs. It is conceivable that aCD28SA on its own only partly activates Tregs and that full activation requires CD103 signaling as a second (costimulatory) signal, as has been suggested in a previous study (Russell et al. 1994). In general, outside-in signaling has been described for CD103 on T-cells in a variety of settings (Hardenberg et al. 2018). For example, CD103/E-cadherin interaction has been shown enhance the cytolytic ability of cytotoxic T-cells through triggering the polarization of lytic granules to the immunological synapse (Le Floc'H et al. 2007). Similarly, CD103/E-cadherin interaction could enhance Treg activation. However, so far is merely a hypothesis derived from correlative evidence. This proposed function of CD103 for Treg activation would not be limited to aCD28SA stimulation, as it was found in the present study that dermal Tregs in CD103$^{-/-}$ mice show diminished FoxP3 expression during the effector phase. As mentioned before FoxP3 expression correlates with Treg activation. This diminished FoxP3 expression could also be explained through the proposed impairment in Treg activation. Impaired Treg activation would also provide a mechanism for the Treg dysfunction during both the sensitization and the effector phase in CD103$^{-/-}$ mice. As a matter of fact, Treg activation was shown to be crucial for the regulation of the sensitization phase and the effector phase by Tregs (Ring et al. 2010a). It must be noted that other studies found that Tregs from CD103$^{-/-}$ mice are fully capable of suppressing T-cell proliferation *in vitro* (Annacker et al. 2005; Suffia et al. 2005). Moreover, Tregs from CD103$^{-/-}$ mice suppressed autoimmune colitis to the same degree as Tregs from wt mice (Annacker et al. 2005). However, based on our findings the detrimental effects of CD103 deficiency on Treg function would only become apparent in the context of *in vivo* activation. Experiments that examine the functionality of *in vivo* activated CD103$^{-/-}$ Tregs might shed further light on this. Tregs isolated from aCD28SA-treated wt and CD103$^{-/-}$ mice could be compared in an *in vitro* suppression assay.

6 Summary

Research leading up to this study found CD103$^{-/-}$ mice to display an increased susceptibility to allergic contact dermatitis. The aim of this study was to determine whether CD103 deficiency causes an impairment in the regulatory function of Tregs and to investigate possible mechanisms.

At first it was studied whether Treg function was impaired during the sensitization phase. For that purpose, Tregs from wt and from CD103$^{-/-}$ mice were injected into Treg-depleted DEREG mice prior to sensitization. It was found that Tregs from wt mice successfully suppressed sensitization, whereas Tregs from CD103$^{-/-}$ mice failed to do not.

Next, CD103$^{-/-}$ Tregs were examined in the effector phase. Tregs from wt mice and from CD103$^{-/-}$ mice were transferred into Rag-1$^{-/-}$ mice which were simultaneously reconstituted with OXA draining lymph node cells to allow the induction of ACD. After elicitation of the effector phase, Tregs from CD103$^{-/-}$ mice were found to be unable to suppress the effector phase, particularly the later stages.

Impaired Treg retention in the skin due to CD103 deficiency is a possible mechanism that could mediate the observed dysfunction. When investigating T-cell retention in the dermis no difference in dermal retention between CD103 competent and CD103 deficient lymphocytes was found 24 hours after intradermal injection. However, this does not exclude an effect at later time points, which were not investigated in this thesis.

In the last part of this thesis it was investigated whether FoxP3 upregulation after Treg activation is disrupted in CD103$^{-/-}$ mice. Wildtype and CD103$^{-/-}$ mice were treated with the superagonistic CD28-directed antibody, D665, a known activator of regulatory T-cells. Strikingly, not only FoxP3 upregulation, but the overall response to the antibody was abrogated in CD103$^{-/-}$ mice. In CD103$^{-/-}$ mice lymph node Tregs failed to expand and adequately upregulate CD25 and FoxP3. This suggests that Treg activation in CD103$^{-/-}$ mice is more broadly impaired.

Taken together, this study showed that Tregs from CD103$^{-/-}$ are dysfunctional in both the sensitization and the effector phase explaining the aggravated CHS response of CD103$^{-/-}$mice. Furthermore, evidence for an impairment of the ability of Tregs in CD103$^{-/-}$ mice to be activated was found. These findings imply that Tregs in CD103$^{-/-}$ mice are fundamentally dysfunctional. Further experiments are needed to elucidate how CD103 controls Treg function. This study shows that CD103 is not only a marker for a Treg subset, but also of significance for Treg function in the context of allergic contact dermatitis.

7 Appendix

7.1 Supplementary data

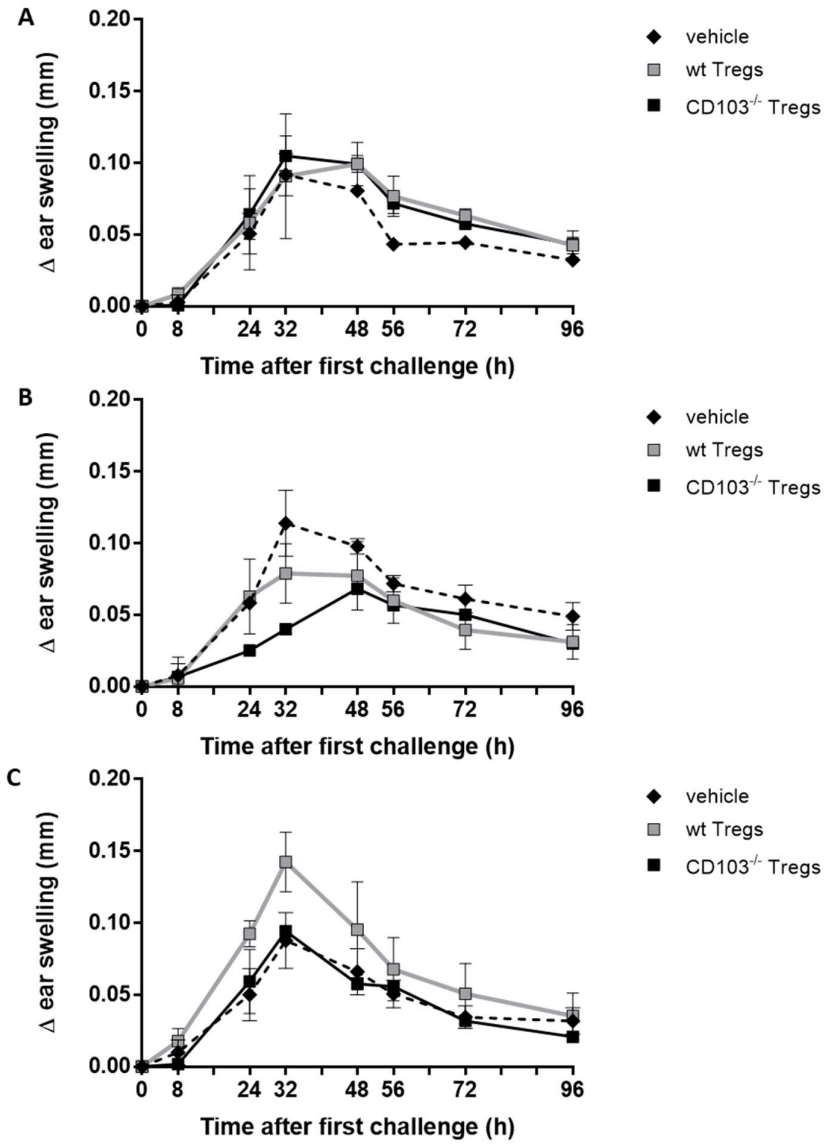

Figure A1: Treg transfers in wt mice prior to sensitization, results of three independent experiments.
$CD4^+$ $CD25^+$ regulatory T-cells (Tregs) were isolated from skin-draining lymph nodes (skin dLN) of wt (wt Tregs) and $CD103^{-/-}$ mice ($CD103^{-/-}$ Tregs) and injected into recipient wt mice ($0.5*10^6$ Tregs per mouse). The standard CHS protocol was initiated the next day through sensitization with 100 µl 3% OXA. After 5 days, the right ears were challenged with 20 µl 1% OXA, while the left ears were treated with 20 µl of vehicle (ethanol). Ear thickness measurements were performed by a blinded experimenter. Data points represent normalized differences in ear thickness between the OXA-treated and the vehicle-treated ears (mean ± SD). **A)** vehicle n = 3; wt Tregs n = 6; $CD103^{-/-}$ Tregs n = 2 **B)** vehicle n = 3; wt Tregs n = 3; $CD103^{-/-}$ Tregs n = 1 **C)** vehicle n = 3; wt Tregs n = 2; $CD103^{-/-}$ Tregs n = 2.

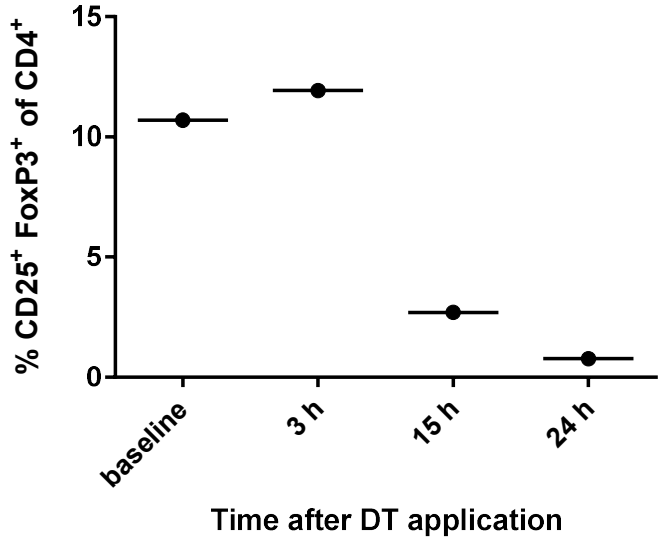

Figure A2: Short-term Treg-recovery kinetic after a single injection of DT
DEREG mice were injected with 1 µg of DT. After different time intervals the mice were killed and the frequency of $CD25^+$ $FoxP3^+$ on living $CD4^+$ cells in dLN cell suspensions was analyzed by flow cytometry. A vehicle-treated DEREG mouse was used to determine the baseline value. The $CD25^+$ $FoxP3^+$ cell frequency of the $CD4^+$ subset is depicted (n=1 per timepoint). A pre-gate was set on living cells.

8 References

Akiba H, Kehren J, Ducluzeau M-T, Krasteva M, Horand F, Kaiserlian D, Kaneko F, Nicolas J-F (2002): Skin Inflammation During Contact Hypersensitivity Is Mediated by Early Recruitment of CD8+ T Cytotoxic 1 Cells Inducing Keratinocyte Apoptosis. J Immunol 168, 3079–3087

Alvarez D, Vollmann EH, Andrian UH von (2008): Mechanisms and Consequences of Dendritic Cell Migration. Immunity 29, 325

Andrews LP, Marciscano AE, Drake CG, Vignali DAA (2017): LAG3 (CD223) as a Cancer Immunotherapy Target. Immunol Rev 276, 80–96

Annacker O, Coombes JL, Malmstrom V, Uhlig HH, Bourne T, Johansson-Lindbom B, Agace WW, Parker CM, Powrie F (2005): Essential role for CD103 in the T cell–mediated regulation of experimental colitis. J Exp Med 202, 1051–1061

Antonopoulos C, Cumberbatch M, Dearman RJ, Daniel RJ, Kimber I, Groves RW (2001): Functional caspase-1 is required for Langerhans cell migration and optimal contact sensitization in mice. J Immunol 166, 3672–3677

Antonopoulos C, Cumberbatch M, Mee JB, Dearman RJ, Wei X-Q, Liew FY, Kimber I, Groves RW (2008): IL-18 is a key proximal mediator of contact hypersensitivity and allergen-induced Langerhans cell migration in murine epidermis. J Leukoc Biol 83, 361–367

Anz D, Müller W, Golic M, Kunz WG, Rapp M, Kölzer VH, Ellermeier J, Ellwart JW, Schnurr M, Bourquin C et al. (2011): CD103 is a hallmark of tumor-infiltrating regulatory T cells. Int J Cancer 129, 2417–2426

Banz A, Peixoto A, Pontoux C, Cordier C, Rocha B, Papiernik M (2003): A unique subpopulation of CD4+ regulatory T cells controls wasting disease, IL-10 secretion and T cell homeostasis. Eur J Immunol 33, 2419–2428

Baroni A, Buommino E, Gregorio V de, Ruocco E, Ruocco V, Wolf R (2012): Structure and function of the epidermis related to barrier properties. Clin Dermatol 30, 257–262

Bäsler K, Brandner JM (2017): Tight junctions in skin inflammation. Pflugers Arch 469, 3–14

Belkaid Y, Piccirillo CA, Mendez S, Shevach EM, Sacks DL (2002): CD4+CD25+ regulatory T cells control Leishmania major persistence and immunity. Nature 420, 502–507

Bennett CL, Christie J, Ramsdell F, Brunkow ME, Ferguson PJ, Whitesell L, Kelly TE, Saulsbury FT, Chance PF, Ochs HD (2001): The immune dysregulation, polyendocrinopathy, enteropathy, X-linked syndrome (IPEX) is caused by mutations of FOXP3. Nat Genet 27, 20–21

Biedermann T, Kneilling M, Mailhammer R, Maier K, Sander CA, Kollias G, Kunkel SL, Hultner L, Rocken M (2000): Mast cells control neutrophil recruitment during T cell-mediated delayed-type hypersensitivity reactions through tumor necrosis factor and macrophage inflammatory protein 2. J Exp Med 192, 1441–1452

Bonneville M, Chavagnac C, Vocanson M, Rozieres A, Benetiere J, Pernet I, Denis A, Nicolas JF, Hennino A (2007): Skin contact irritation conditions the development and severity of allergic contact dermatitis. J Invest Dermatol 127, 1430–1435

Bos JD, Meinardi MM (2000): The 500 Dalton rule for the skin penetration of chemical compounds and drugs. Exp Dermatol 9, 165–169

Bour H, Peyron E, Gaucherand M, Garrigue JL, Desvignes C, Kaiserlian D, Revillard JP, Nicolas JF (1995): Major histocompatibility complex class I-restricted CD8+ T cells and class II-restricted CD4+ T cells, respectively, mediate and regulate contact sensitivity to dinitrofluorobenzene. Eur J Immunol 25, 3006–3010

Boyman O, Sprent J (2012): The role of interleukin-2 during homeostasis and activation of the immune system. Nat Rev Immunol 12, 180

Brasch J, Becker D, Aberer W, Bircher A, Kränke B, Jung K, Przybilla B, Biedermann T, Werfel T, John SM et al. (2014): Guideline contact dermatitis: S1-Guidelines of the German Contact Allergy Group (DKG) of the German Dermatology Society (DDG), the Information Network of Dermatological Clinics (IVDK), the German Society for Allergology and Clinical Immunology (DGAKI), the Working Group for Occupational and Environmental Dermatology (ABD) of the DDG, the Medical Association of German Allergologists (AeDA), the Professional Association of German Dermatologists (BVDD) and the DDG. Allergo J Int 23, 126–138

Braun A, Dewert N, Brunnert F, Schnabel V, Hardenberg J-H, Richter B, Zachmann K, Cording S, Claßen A, Brans R et al. (2015): Integrin αE(CD103) Is Involved in Regulatory T-Cell Function in Allergic Contact Hypersensitivity. J Invest Dermatol 135, 2982–2991

Brown, Furness, Speight, Thomas, Li, Thornhill, Farthing (1999): Mechanisms of binding of cutaneous lymphocyte-associated antigen-positive and alphaebeta7-positive lymphocytes to oral and skin keratinocytes. Immunology 98, 9–15

Brunkow ME, Jeffery EW, Hjerrild KA, Paeper B, Clark LB, Yasayko SA, Wilkinson JE, Galas D, Ziegler SF, Ramsdell F (2001): Disruption of a new forkhead/winged-helix protein, scurfin, results in the fatal lymphoproliferative disorder of the scurfy mouse. Nat Genet 27, 68–73

Bundesanstalt für Arbeitsschutz und Arbeitsmedizin: Sicherheit und Gesundheit bei der Arbeit 2015; Bundesministerium für Arbeit und Soziales (BMAS) in Zusammenarbeit mit Bundesanstalt für Arbeitsschutz und Arbeitsmedizin (BAuA) 2016, Dortmund 2016

Campos RA, Szczepanik M, Itakura A, Akahira-Azuma M, Sidobre S, Kronenberg M, Askenase PW (2003): Cutaneous immunization rapidly activates liver invariant Valpha14 NKT cells stimulating B-1 B cells to initiate T cell recruitment for elicitation of contact sensitivity. J Exp Med 198, 1785–1796

Campos RA, Szczepanik M, Itakura A, Lisbonne M, Dey N, Leite-de-Moraes MC, Askenase PW (2006): Interleukin-4-dependent innate collaboration between iNKT cells and B-1 B cells controls adaptative contact sensitivity. Immunology 117, 536–547

Cepek KL, Shaw SK, Parker CM, Russell GJ, Morrow JS, Rimm DL, Brenner MB (1994): Adhesion between epithelial cells and T lymphocytes mediated by E-cadherin and the alpha E beta 7 integrin Nature 372, 190–193

Chang L-Y, Lin Y-C, Kang C-W, Hsu C-Y, Chu Y-Y, Huang C-T, Day Y-J, Chen T-C, Yeh C-T, Lin C-Y (2012): The Indispensable Role of CCR5 for In Vivo Suppressor Function of Tumor-Derived CD103+ Effector/Memory Regulatory T Cells. J Immunol 189, 567–574

Chen X, Oppenheim JJ (2011): Resolving the identity myth: key markers of functional CD4+FoxP3+ regulatory T cells. Int Immunopharmacol 11, 1489–1496

Chenna Narendra S, Chalise JP, Biggs S, Kalinke U, Magnusson M (2018): Regulatory T-Cells Mediate IFN-alpha-Induced Resistance against Antigen-Induced Arthritis. Front Immunol 9, 285

Chinen T, Kannan AK, Levine AG, Fan X, Klein U, Zheng Y, Gasteiger G, Feng Y, Fontenot JD, Rudensky AY (2016): An essential role for IL-2 receptor in regulatory T cell function. Nat Immunol 17, 1322–1333

Chipinda I, Hettick JM, Siegel PD (2011): Haptenation: chemical reactivity and protein binding. J Allergy (Cairo) 2011, 839682

Corgnac S, Boutet M, Kfoury M, Naltet C, Mami-Chouaib F (2018): The Emerging Role of CD8+ Tissue Resident Memory T (TRM) Cells in Antitumor Immunity: A Unique Functional Contribution of the CD103 Integrin. Front Immunol 1904

Couper KN, Blount DG, Souza JB de, Suffia I, Belkaid Y, Riley EM (2007): Incomplete depletion and rapid regeneration of Foxp3+ regulatory T cells following anti-CD25 treatment in malaria-infected mice. J Immunol 178, 4136–4146

Cumberbatch M, Kimber I (1995): Tumour necrosis factor-alpha is required for accumulation of dendritic cells in draining lymph nodes and for optimal contact sensitization. Immunology 84, 31–35

Cumberbatch M, Dearman RJ, Kimber I (1997): Langerhans cells require signals from both tumour necrosis factor-alpha and interleukin-1 beta for migration. Immunology 92, 388–395

Cumberbatch M, Griffiths CE, Tucker SC, Dearman RJ, Kimber I (1999): Tumour necrosis factor-alpha induces Langerhans cell migration in humans. Br J Dermatol 141, 192–200

Dalod M, Chelbi R, Malissen B, Lawrence T (2014): Dendritic cell maturation: functional specialization through signaling specificity and transcriptional programming. EMBO J 33, 1104–1116

Deaglio S, Dwyer KM, Gao W, Friedman D, Usheva A, Erat A, Chen JF, Enjyoji K, Linden J, Oukka M et al. (2007): Adenosine generation catalyzed by CD39 and CD73 expressed on regulatory T cells mediates immune suppression. J Exp Med 204, 1257–1265

del Rio M-L, Bernhardt G, Rodriguez-Barbosa J-I, Forster R (2010): Development and functional specialization of CD103+ dendritic cells. Immunol Rev 234, 268–281

Dennehy KM, Elias F, Zeder-Lutz G, Ding X, Altschuh D, Luhder F, Hünig T (2006): Cutting Edge: Monovalency of CD28 Maintains the Antigen Dependence of T Cell Costimulatory Responses. J Immunol 176, 5725–5729

Dickel H, Kuss O, Blesius CR, Schmidt A, Diepgen TL (2001): Occupational skin diseases in Northern Bavaria between 1990 and 1999: a population-based study. Br J Dermatol 145, 453–462

Divkovic M, Pease CK, Gerberick GF, Basketter DA (2005): Hapten–protein binding: from theory to practical application in the in vitro prediction of skin sensitization. Contact Dermatitis 53, 189–200

Dudda JC, Perdue N, Bachtanian E, Campbell DJ (2008): Foxp3+ regulatory T cells maintain immune homeostasis in the skin. J Exp Med 205, 1559–1565

Dudeck A, Dudeck J, Scholten J, Petzold A, Surianarayanan S, Köhler A, Peschke K, Vöhringer D, Waskow C, Krieg T et al. (2011): Mast Cells Are Key Promoters of Contact Allergy that Mediate the Adjuvant Effects of Haptens. Immunity 34, 973–984

Duhen T, Duhen R, Montler R, Moses J, Moudgil T, Miranda NF de, Goodall CP, Blair TC, Fox BA, McDermott JE et al. (2018): Co-expression of CD39 and CD103 identifies tumor-reactive CD8 T cells in human solid tumors. Nat Commun 9, 2724

Egawa G, Honda T, Tanizaki H, Doi H, Miyachi Y, Kabashima K (2011): In Vivo Imaging of T-Cell Motility in the Elicitation Phase of Contact Hypersensitivity Using Two-Photon Microscopy. J Invest Dermatol 131, 977–979

Engeman T, Gorbachev AV, Kish DD, Fairchild RL (2004): The intensity of neutrophil infiltration controls the number of antigen-primed CD8 T cells recruited into cutaneous antigen challenge sites. J Leukoc Biol 76, 941–949

Esser PR, Wölfle U, Dürr C, Löwenich FD von, Schempp CM, Freudenberg MA, Jakob T, Martin SF (2012): Contact Sensitizers Induce Skin Inflammation via ROS Production and Hyaluronic Acid Degradation. PLoS One 7, e41340

Fear VS, Lai SP, Zosky GR, Perks KL, Gorman S, Blank F, Garnier C von, Stumbles PA, Strickland DH (2016): A pathogenic role for the integrin CD103 in experimental allergic airways disease. Physiol Rep 4, e13021

Fontenot JD, Gavin MA, Rudensky AY (2003): Foxp3 programs the development and function of CD4+CD25+ regulatory T cells. Nat Immunol 4, 330–336

Furuse M, Hata M, Furuse K, Yoshida Y, Haratake A, Sugitani Y, Noda T, Kubo A, Tsukita S (2002): Claudin-based tight junctions are crucial for the mammalian epidermal barrier: a lesson from claudin-1-deficient mice. J Cell Biol 156, 1099–1111

Gocinski BL, Tigelaar RE (1990): Roles of CD4+ and CD8+ T cells in murine contact sensitivity revealed by in vivo monoclonal antibody depletion. J Immunol 144, 4121–4128

Gogishvili T, Langenhorst D, Luhder F, Elias F, Elflein K, Dennehy KM, Gold R, Hünig T (2009): Rapid regulatory T-cell response prevents cytokine storm in CD28 superagonist treated mice. PLoS One 4, e4643

Gondek DC, Lu L-F, Quezada SA, Sakaguchi S, Noelle RJ (2005): Cutting Edge: Contact-Mediated Suppression by CD4+CD25+ Regulatory Cells Involves a Granzyme B-Dependent, Perforin-Independent Mechanism. J Immunol 174, 1783–1786

Grabbe S, Steinert M, Mahnke K, Schwartz A, Luger TA, Schwarz T (1996): Dissection of antigenic and irritative effects of epicutaneously applied haptens in mice. Evidence that not the antigenic component but nonspecific proinflammatory effects of haptens determine the concentration-dependent elicitation of allergic contact dermatitis. J Clin Invest 98, 1158–1164

Griem P, Panthel K, Kalbacher H, Gleichmann E (1996): Alteration of a model antigen by Au(III) leads to T cell sensitization to cryptic peptides. Eur J Immunol 26, 279–287

Harari OA, McHale JF, Marshall D, Ahmed S, Brown D, Askenase PW, Haskard DO (1999): Endothelial Cell E- and P-Selectin Up-Regulation in Murine Contact Sensitivity Is Prolonged by Distinct Mechanisms Occurring in Sequence. J Immunol 163, 6860–6866

Hardenberg J-HB, Braun A, Schön MP (2018): A Yin and Yang in Epithelial Immunology: The Roles of the alphaE(CD103)beta7 Integrin in T Cells. J Invest Dermatol 138, 23–31

Harding FA, McArthur JG, Gross JA, Raulet DH, Allison JP (1992): CD28-mediated signalling costimulates murine T cells and prevents induction of anergy in T-cell clones. Nature 356, 607–609

Higgins JM, Mandlebrot DA, Shaw SK, Russell GJ, Murphy EA, Chen YT, Nelson WJ, Parker CM, Brenner MB (1998): Direct and regulated interaction of integrin alphaEbeta7 with E-cadherin. J Cell Biol 140, 197–210

Homey B, Alenius H, Müller A, Soto H, Bowman EP, Yuan W, McEvoy L, Lauerma AI, Assmann T, Bunemann E et al. (2002): CCL27-CCR10 interactions regulate T cell-mediated skin inflammation. Nat Med 8, 157–165

Honda T, Otsuka A, Tanizaki H, Minegaki Y, Nagao K, Waldmann H, Tomura M, Hori S, Miyachi Y, Kabashima K (2011): Enhanced murine contact hypersensitivity by depletion of endogenous regulatory T cells in the sensitization phase. J Dermatol Sci 61, 144–147

Honda T, Egawa G, Grabbe S, Kabashima K (2013): Update of Immune Events in the Murine Contact Hypersensitivity Model: Toward the Understanding of Allergic Contact Dermatitis. J Invest Dermatol 133, 303–315

Honda T, Kabashima K (2016): Novel concept of iSALT (inducible skin-associated lymphoid tissue) in the elicitation of allergic contact dermatitis. Proc Jpn Acad Ser B Phys Biol Sci 92, 20–28

Hori S, Nomura T, Sakaguchi S (2003): Control of regulatory T cell development by the transcription factor Foxp3. Science 299, 1057–1061

Hühn J, Siegmund K, Lehmann JCU, Siewert C, Haubold U, Feuerer M, Debes GF, Lauber J, Frey O, Przybylski GK et al. (2004): Developmental Stage, Phenotype, and Migration Distinguish Naive- and Effector/Memory-like CD4+ Regulatory T Cells. J Exp Med 199, 303–313

Hünig T, Dennehy K (2005): CD28 superagonists: mode of action and therapeutic potential. Immunol Lett 100, 21–28

Jenkinson SE, Whawell SA, Swales BM, Corps EM, Kilshaw PJ, Farthing PM (2011): The αE(CD103)β7 integrin interacts with oral and skin keratinocytes in an E-cadherin-independent manner. Immunology 132, 188–196

Karecla PI, Bowden SJ, Green SJ, Kilshaw PJ (1995): Recognition of E-cadherin on epithelial cells by the mucosal T cell integrin alpha M290 beta 7 (alpha E beta 7). Eur J Immunol 25, 852–856

Kehren J, Desvignes C, Krasteva M, Ducluzeau MT, Assossou O, Horand F, Hahne M, Kägi D, Kaiserlian D, Nicolas JF (1999): Cytotoxicity Is Mandatory for CD8+ T Cell–mediated Contact Hypersensitivity. J Exp Med 189, 779–786

Kim JM, Rasmussen JP, Rudensky AY (2007): Regulatory T cells prevent catastrophic autoimmunity throughout the lifespan of mice. Nat Immunol 8, 191–197

Kish DD, Gorbachev AV, Fairchild RL (2005): CD8+ T cells produce IL-2, which is required for CD4+CD25+ T cell regulation of effector CD8+ T cell development for contact hypersensitivity responses. J Leukoc Biol 78, 725–735

Kish DD, Li X, Fairchild RL (2009): CD8 T cells producing IL-17 and IFN-γ initiate the innate immune response required for response to antigen skin challenge. J Immunol 182, 5949–5959

Kish DD, Volokh N, Baldwin WM, Fairchild RL (2011): Hapten Application to the Skin Induces an Inflammatory Program Directing Hapten-Primed Effector CD8 T Cell Interaction with Hapten-Presenting Endothelial Cells. J Immunol 186, 2117–2126

Klages K, Mayer CT, Lahl K, Loddenkemper C, Teng MWL, Ngiow SF, Smyth MJ, Hamann A, Hühn J, Sparwasser T (2010): Selective depletion of Foxp3+ regulatory T cells improves effective therapeutic vaccination against established melanoma. Cancer Res 70, 7788–7799

Kondo S, Kooshesh F, Wang B, Fujisawa H, Sauder DN (1996): Contribution of the CD28 molecule to allergic and irritant-induced skin reactions in CD28 -/- mice. J Immunol 157, 4822–4829

Konkel JE, Zhang D, Zanvit P, Chia C, Zangarle-Murray T, Jin W, Wang S, Chen W (2017): Transforming Growth Factor-β Signaling in Regulatory T Cells Controls T Helper-17 Cells and Tissue-Specific Immune Responses. Immunity 46, 660–674

Lahl K, Loddenkemper C, Drouin C, Freyer J, Arnason J, Eberl G, Hamann A, Wagner H, Hühn J, Sparwasser T (2007): Selective depletion of Foxp3+ regulatory T cells induces a scurfy-like disease. J Exp Med 204, 57–63

Lahl K, Sparwasser T (2011): In vivo depletion of FoxP3+ Tregs using the DEREG mouse model. Methods Mol Biol 707, 157–172

Landsteiner K, Jacobs J (1936): STUDIES ON THE SENSITIZATION OF ANIMALS WITH SIMPLE CHEMICAL COMPOUNDS. II. J Exp Med 64, 625–639

Lass C, Merfort I, Martin SF (2010): In vitro and in vivo analysis of pro- and anti-inflammatory effects of weak and strong contact allergens. Exp Dermatol 19, 1007–1013

Le Floc'H A, Jalil A, Vergnon I, Le Chansac BM, Lazar V, Bismuth G, Chouaib S, Mami-Chouaib F (2007): αEβ7 integrin interaction with E-cadherin promotes antitumor CTL activity by triggering lytic granule polarization and exocytosis. J Exp Med 204, 559–570

Lehmann J, Hühn J, La Rosa M de, Maszyna F, Kretschmer U, Krenn V, Brunner M, Scheffold A, Hamann A (2002): Expression of the integrin αEβ7 identifies unique subsets of CD25+ as well as CD25− regulatory T cells. Proc Natl Acad Sci U S A 99, 13031–13036

Lehtimäki S, Savinko T, Lahl K, Sparwasser T, Wolff H, Lauerma A, Alenius H, Fyhrquist N (2012): The temporal and spatial dynamics of Foxp3+ Treg cell-mediated suppression during contact hypersensitivity responses in a murine model. J Invest Dermatol 132, 2744–2751

Lin C-H, Hünig T (2003): Efficient expansion of regulatory T cells in vitro and in vivo with a CD28 superagonist. Eur J Immunol 33, 626–638

Lin Y-C, Chang L-Y, Huang C-T, Peng H-M, Dutta A, Chen T-C, Yeh C-T, Lin C-Y (2009): Effector/Memory but Not Naive Regulatory T Cells Are Responsible for the Loss of Concomitant Tumor Immunity. J Immunol 182, 6095–6104

Mackay LK, Rahimpour A, Ma JZ, Collins N, Stock AT, Hafon M-L, Vega-Ramos J, Lauzurica P, Mueller SN, Stefanovic T et al. (2013): The developmental pathway for CD103+CD8+ tissue-resident memory T cells of skin. Nat Immunol 14, 1294–1301

Madison KC (2003): Barrier Function of the Skin: "La Raison d'Être" of the Epidermis. J Invest Dermatol 121, 231–241

Mahnke K, Useliene J, Ring S, Kage P, Jendrossek V, Robson SC, Bylaite-Bucinskiene M, Steinbrink K, Enk AH (2017): Down-Regulation of CD62L Shedding in T Cells by CD39+ Regulatory T Cells Leads to Defective Sensitization in Contact Hypersensitivity Reactions. J Invest Dermatol 137, 106–114

Martin SF, Dudda JC, Bachtanian E, Lembo A, Liller S, Dürr C, Heimesaat MM, Bereswill S, Fejer G, Vassileva R et al. (2008): Toll-like receptor and IL-12 signaling control susceptibility to contact hypersensitivity. J Exp Med 205, 2151–2162

Mayer CT, Ghorbani P, Kuhl AA, Stuve P, Hegemann M, Berod L, Gershwin ME, Sparwasser T (2014): Few Foxp3(+) regulatory T cells are sufficient to protect adult mice from lethal autoimmunity. Eur J Immunol 44, 2990–3002

McHale JF, Harari OA, Marshall D, Haskard DO (1999): Vascular Endothelial Cell Expression of ICAM-1 and VCAM-1 at the Onset of Eliciting Contact Hypersensitivity in Mice: Evidence for a Dominant Role of TNF-α. J Immunol 162, 1648–1655

Micklem KJ, Dong Y, Willis A, Pulford KA, Visser L, Dürkop H, Poppema S, Stein H, Mason DY (1991): HML-1 antigen on mucosa-associated T cells, activated cells, and hairy leukemic cells is a new integrin containing the beta 7 subunit. Am J Pathol 139, 1297–1301

Mokrani M'B, Klibi J, Bluteau D, Bismuth G, Mami-Chouaib F (2014): Smad and NFAT Pathways Cooperate To Induce CD103 Expression in Human CD8 T Lymphocytes. J Immunol 192, 2471–2479

Mombaerts P, Iacomini J, Johnson RS, Herrup K, Tonegawa S, Papaioannou VE (1992): RAG-1-deficient mice have no mature B and T lymphocytes. Cell 68, 869–877

Moore KW, Waal Malefyt R de, Coffman RL, O'Garra A (2001): Interleukin-10 and the interleukin-10 receptor. Annu Rev Immunol 19, 683–765

Natsuaki Y, Egawa G, Nakamizo S, Ono S, Hanakawa S, Okada T, Kusuba N, Otsuka A, Kitoh A, Honda T et al. (2014): Perivascular leukocyte clusters are essential for efficient activation of effector T cells in the skin. Nat Immunol 15, 1064–1069

Pauls K, Schön M, Kubitza RC, Homey B, Wiesenborn A, Lehmann P, Ruzicka T, Parker CM, Schön MP (2001): Role of Integrin αE(CD103)β7 for Tissue-Specific Epidermal Localization of CD8+ T Lymphocytes. J Invest Dermatol 117, 569–575

Peiser M (2013): Role of Th17 Cells in Skin Inflammation of Allergic Contact Dermatits. Clin Dev Immunol 2013

Proksch E, Brandner JM, Jensen J-M (2008): The skin: an indispensable barrier. Exp Dermatol 17, 1063–1072

Raghavan B, Martin SF, Esser PR, Göbeler M, Schmidt M (2012): Metal allergens nickel and cobalt facilitate TLR4 homodimerization independently of MD2. EMBO Rep 13, 1109–1115

Reduta T, Bacharewicz J, Pawłoś A (2013): Patch test results in patients with allergic contact dermatitis in the Podlasie region. Postepy Dermatol Alergol 30, 350–357

Reiser H, Schneeberger EE (1996): Expression and function of B7-1 and B7-2 in hapten-induced contact sensitivity. Eur J Immunol 26, 880–885

Ring S, Schäfer SC, Mahnke K, Lehr HA, Enk AH (2006): CD4+ CD25+ regulatory T cells suppress contact hypersensitivity reactions by blocking influx of effector T cells into inflamed tissue. Eur J Immunol 36, 2981–2992

Ring S, Oliver SJ, Cronstein BN, Enk AH, Mahnke K (2009): CD4+CD25+ regulatory T cells suppress contact hypersensitivity reactions through a CD39, adenosine-dependent mechanism. J Allergy Clin Immunol 123, 1287-96.e2

Ring S, Enk AH, Mahnke K (2010a): ATP Activates Regulatory T Cells In Vivo during Contact Hypersensitivity Reactions. J Immunol 184, 3408–3416

Ring S, Karakhanova S, Johnson T, Enk AH, Mahnke K (2010b): Gap junctions between regulatory T cells and dendritic cells prevent sensitization of CD8(+) T cells. J Allergy Clin Immunol 125, 237-46.e1-7

Ring S, Pushkarevskaya A, Schild H, Probst HC, Jendrossek V, Wirsdorfer F, Ledent C, Robson SC, Enk AH, Mahnke K (2015): Regulatory T cell-derived adenosine induces dendritic cell migration through the Epac-Rap1 pathway. J Immunol 194, 3735–3744

Robinson PW, Green SJ, Carter C, Coadwell J, Kilshaw PJ (2001): Studies on transcriptional regulation of the mucosal T-cell integrin alphaEbeta7 (CD103). Immunology 103, 146–154

Roediger B, Kyle R, Yip KH, Sumaria N, Guy TV, Kim BS, Mitchell AJ, Tay SS, Jain R, Forbes-Blom E et al. (2013): Cutaneous immuno-surveillance and regulation of inflammation by group 2 innate lymphoid cells. Nat Immunol 14, 564–573

Russell GJ, Parker CM, Cepek KL, Mandelbrot DA, Sood A, Mizoguchi E, Ebert EC, Brenner MB, Bhan AK (1994): Distinct structural and functional epitopes of the alpha E beta 7 integrin. Eur J Immunol 24, 2832–2841

Sakaguchi S, Sakaguchi N, Asano M, Itoh M, Toda M (1995): Immunologic self-tolerance maintained by activated T cells expressing IL-2 receptor alpha-chains (CD25). Breakdown of a single mechanism of self-tolerance causes various autoimmune diseases. J Immunol 155, 1151–1164

Sakaguchi S, Miyara M, Costantino CM, Hafler DA (2010): FOXP3+ regulatory T cells in the human immune system. Nat Rev Immunol 10, 490–500

Schäfer L (2014): Complexity of Danger: The Diverse Nature of Damage-associated Molecular Patterns. J Biol Chem 289, 35237–35245

Schlickum S, Sennefelder H, Friedrich M, Harms G, Lohse MJ, Kilshaw P, Schön MP (2008): Integrin αE(CD103)β7 influences cellular shape and motility in a ligand-dependent fashion. Blood 112, 619–625

Schmidt M, Raghavan B, Müller V, Vogl T, Fejer G, Tchaptchet S, Keck S, Kalis C, Nielsen PJ, Galanos C et al. (2010): Crucial role for human Toll-like receptor 4 in the development of contact allergy to nickel. Nat Immunol 11, 814–819

Schön MP, Arya A, Murphy EA, Adams CM, Strauch UG, Agace WW, Marsal J, Donohue JP, Her H, Beier DR et al. (1999): Mucosal T Lymphocyte Numbers Are Selectively Reduced in Integrin αE (CD103)-Deficient Mice. J Immunol 162, 6641–6649

Schön MP, Schön M, Warren HB, Donohue JP, Parker CM (2000): Cutaneous Inflammatory Disorder in Integrin αE (CD103)-Deficient Mice. J Immunol 165, 6583–6589

Sebastiani S, Albanesi C, De PO, Puddu P, Cavani A, Girolomoni G (2002): The role of chemokines in allergic contact dermatitis. Arch Dermatol Res 293, 552–559

Shornick LP, Togni P de, Mariathasan S, Göllner J, Strauss-Schönberger J, Karr RW, Ferguson TA, Chaplin DD (1996): Mice deficient in IL-1beta manifest impaired contact hypersensitivity to trinitrochlorobenzone. J Exp Med 183, 1427–1436

Siewert C, Lauer U, Cording S, Bopp T, Schmitt E, Hamann A, Hühn J (2008): Experience-Driven Development: Effector/Memory-Like αE+Foxp3+ Regulatory T Cells Originate from Both Naive T Cells and Naturally Occurring Naive-Like Regulatory T Cells. J Immunol 180, 146–155

Strauch UG, Mueller RC, Li XY, Cernadas M, Higgins JMG, Binion DG, Parker CM (2001): Integrin E(CD103) 7 Mediates Adhesion to Intestinal Microvascular Endothelial Cell Lines Via an E-Cadherin-Independent Interaction. J Immunol 166, 3506–3514

Suffia I, Reckling SK, Salay G, Belkaid Y (2005): A Role for CD103 in the Retention of CD4+CD25+ Treg and Control of Leishmania major Infection. J Immunol 174, 5444–5455

Suntharalingam G, Perry MR, Ward S, Brett SJ, Castello-Cortes A, Brunner MD, Panoskaltsis N (2006): Cytokine Storm in a Phase 1 Trial of the Anti-CD28 Monoclonal Antibody TGN1412. N Engl J Med 355, 1018–1028

Sutterwala FS, Ogura Y, Szczepanik M, Lara-Tejero M, Lichtenberger GS, Grant EP, Bertin J, Coyle AJ, Galán JE, Askenase PW et al. (2006): Critical Role for NALP3/CIAS1/Cryopyrin in Innate and Adaptive Immunity through Its Regulation of Caspase-1. Immunity 24, 317–327

Teng MWL, Ngiow SF, Scheidt B von, McLaughlin N, Sparwasser T, Smyth MJ (2010): Conditional regulatory T-cell depletion releases adaptive immunity preventing carcinogenesis and suppressing established tumor growth. Cancer Res 70, 7800–7809

Thyssen JP, Linneberg A, Menné T, Johansen JD (2007): The epidemiology of contact allergy in the general population – prevalence and main findings. Contact Dermatitis 57, 287–299

Tohyama M, Shirakara Y, Yamasaki K, Sayama K, Hashimoto K (2001): Differentiated keratinocytes are responsible for TNF-alpha regulated production of macrophage inflammatory protein 3alpha/CCL20, a potent chemokine for Langerhans cells. J Dermatol Sci 27, 130–139

Tomura M, Honda T, Tanizaki H, Otsuka A, Egawa G, Tokura Y, Waldmann H, Hori S, Cyster JG, Watanabe T et al. (2010): Activated regulatory T cells are the major T cell type emigrating from the skin during a cutaneous immune response in mice. J Clin Invest 120, 883–893

Traidl C, Sebastiani S, Albanesi C, Merk HF, Puddu P, Girolomoni G, Cavani A (2000): Disparate cytotoxic activity of nickel-specific CD8+ and CD4+ T cell subsets against keratinocytes. J Immunol 165, 3058–3064

Trautmann A, Akdis M, Kleemann D, Altznauer F, Simon H-U, Graeve T, Noll M, Bröcker E-B, Blaser K, Akdis CA (2000): T cell–mediated Fas-induced keratinocyte apoptosis plays a key pathogenetic role in eczematous dermatitis. J Clin Invest 106, 25–35

Tsuji RF, Szczepanik M, Kawikova I, Paliwal V, Campos RA, Itakura A, Akahira-Azuma M, Baumgarth N, La Herzenberg, Askenase PW (2002): B Cell–dependent T Cell Responses: IgM Antibodies Are Required to Elicit Contact Sensitivity. J Exp Med 196, 1277–1290

Uter W, Ramsch C, Aberer W, Ayala F, Balato A, Beliauskiene A, Fortina AB, Bircher A, Brasch J, Chowdhury MMU et al. (2009): The European baseline series in 10 European Countries, 2005/2006--results of the European Surveillance System on Contact Allergies (ESSCA). Contact Dermatitis 61, 31–38

Vignali DAA, Collison LW, Workman CJ (2008): How regulatory T cells work. Nat Rev Immunol 8, 523–532

Vocanson M, Hennino A, Cluzel-Tailhardat M, Saint-Mezard P, Benetiere J, Chavagnac C, Berard F, Kaiserlian D, Nicolas JF (2006): CD8+ T cells are effector cells of contact dermatitis to common skin allergens in mice. J Invest Dermatol 126, 815–820

Vocanson M, Hennino A, Rozières A, Poyet G, Nicolas J-F (2009): Effector and regulatory mechanisms in allergic contact dermatitis. Allergy 64, 1699–1714

Walsh KP, Mills KHG (2013): Dendritic cells and other innate determinants of T helper cell polarisation. Trends Immunol 34, 521–530

Walunas TL, Lenschow DJ, Bakker CY, Linsley PS, Freeman GJ, Green JM, Thompson CB, Bluestone JA (1994): CTLA-4 can function as a negative regulator of T cell activation. Immunity 1, 405–413

Wan YY, Flavell RA (2007): Regulatory T-cell functions are subverted and converted owing to attenuated Foxp3 expression. Nature 445, 766–770

Watanabe H, Gaide O, Pétrilli V, Martinon F, Contassot E, Roques S, Kummer JA, Tschopp J, French LE (2007): Activation of the IL-1β-Processing Inflammasome Is Involved in Contact Hypersensitivity. J Invest Dermatol 127, 1956–1963

Watanabe H, Gehrke S, Contassot E, Roques S, Tschopp J, Friedmann PS, French LE, Gaide O (2008): Danger Signaling through the Inflammasome Acts as a Master Switch between Tolerance and Sensitization. J Immunol 180, 5826–5832

Weber FC, Esser PR, Müller T, Ganesan J, Pellegatti P, Simon MM, Zeiser R, Idzko M, Jakob T, Martin SF (2010): Lack of the purinergic receptor P2X(7) results in resistance to contact hypersensitivity. J Exp Med 207, 2609–2619

Weber FC, Németh T, Csepregi JZ, Dudeck A, Roers A, Ozsvári B, Oswald E, Puskás LG, Jakob T, Mócsai A et al. (2015): Neutrophils are required for both the sensitization and elicitation phase of contact hypersensitivity. J Exp Med 212, 15–22

Weltzien HU, Moulon C, Martin S, Padovan E, Hartmann U, Kohler J (1996): T cell immune responses to haptens. Structural models for allergic and autoimmune reactions. Toxicology 107, 141–151

Xu H, DiIulio NA, Fairchild RL (1996): T cell populations primed by hapten sensitization in contact sensitivity are distinguished by polarized patterns of cytokine production: interferon gamma-producing (Tc1) effector CD8+ T cells and interleukin (Il) 4/Il-10-producing (Th2) negative regulatory CD4+ T cells. J Exp Med 183, 1001–1012

Yardeni T, Eckhaus M, Morris HD, Huizing M, Hoogstraten-Miller S (2011): Retro-orbital injections in mice. Lab Anim (NY) 40, 155–160

Yuan X, Dee MJ, Altman NH, Malek TR (2015): IL-2Rβ–Dependent Signaling and CD103 Functionally Cooperate To Maintain Tolerance in the Gut Mucosa. J Immunol 194, 1334–1346